

[Click here to view linked References](#)

1 **1 Quantification of chlorophyll *a*, chlorophyll *b* and pheopigments *a* in lake**
2 **2 sediments through deconvolution of bulk UV-VIS absorption spectra**

3
4
5 3
6
7
8 4 Andrea Sanchini^{1,2*}, Martin Grosjean^{1,2}

9
10 5 ¹ Oeschger Centre for Climate Change Research, University of Bern, 3012 Bern,
11 6 Switzerland

12
13 7 ² Institute of Geography, University of Bern, Hallerstrasse 12, 3012 Bern, Switzerland

14
15
16 8
17
18 9 ***Corresponding author:**

19
20 10
21 11 Andrea Sanchini
22 12 University of Bern
23 13 Hallerstrasse 12
24 14 3012 Bern, Switzerland
25 15 andrea.sanchini@giub.unibe.ch

26
27
28 16
29 17 **Co-Author:**

30
31 18
32 19 Martin Grosjean
33 20 martin.grosjean@oeschger.unibe.ch

34
35 21
36 22 **Keywords:**

37
38
39 23
40 24 Sedimentary pigments, UV-VIS absorption spectra, Deconvolution, Aquatic
41 25 paleoproduction, chlorophyll preservation index

42
43
44
45
46
47
48
49
50
51
52
53
54
55
56
57
58
59
60
61
62
63
64
65

32 **Abstract**

33

34 Assessments of aquatic paleoproduction and pigment preservation require accurate
35 identification and quantification of sedimentary chlorophylls. Using chromatographic
36 techniques to analyze long records at high-resolution is impractical because they are
37 expensive and labor intensive. We have developed a new rapid and low-cost approach to
38 infer the concentrations of chlorophyll *a*, chlorophyll *b* and related chlorophyll
39 derivatives (pheopigments *a*) from the mathematical decomposition of UV-VIS measured
40 bulk spectrophotometer absorption spectra of standard solutions and sediment extracts.
41 We validated our method against high-performance liquid chromatography (HPLC)
42 measurements on standard solutions and on varved, anoxic sediment from eutrophic Lake
43 Lugano (Ponte Tresa sub-basin, southern Switzerland), where the history of productivity
44 is relatively well known for the 20th century. Our mathematical approach quantifies the
45 concentration of chlorophyll *b* ($R_{\text{adj}}^2 = 0.99$, RMSEP $\sim 5.9\%$), chlorophyll *a* ($R_{\text{adj}}^2 = 0.98$,
46 RMSEP $\sim 5.0\%$), and pyropheophorbide *a* ($R_{\text{adj}}^2 = 0.99$, RMSEP $\sim 7.8\%$) in standard
47 solutions. We obtain comparable results for total chloropigment *a* (chlorophyll *a* +
48 pheopigments *a*), chlorophyll *a* and diagenetic products (pheopigments *a*) in the sediment
49 samples of our case study (Ponte Tresa). Here, HPLC concentrations of chlorophyll *b*
50 were very too. The method has, however, the potential to achieve values for chlorophyll
51 *b* concentrations in sediments with chlorophylls *a*/chlorophylls *b* ratios lower than 3.4.
52 The pigment stratigraphy of the Ponte Tresa sediments correspond very well with the
53 paleoproduction and eutrophication history of the 20th century. The ratio between
54 chlorophyll *a* and pheopigments *a* used as a qualitative indicator of sedimentary
55 chlorophyll preservation (chlorophyll *a*/\{chlorophyll *a*+pheopigments *a*\}) is only weakly
56 correlated with aquatic paleoproduction ($r_{\text{adj}} = 0.35$, p-value = 0.045) and remained
57 remarkably constant in the recent century despite strong anthropogenic eutrophication.
58 The new method is useful for obtaining, in a cost- and time-efficient way, information
59 about major sedimentary pigment groups which are relevant to infer paleoproduction,
60 potentially green algae biomass, pigment preservation and early diagenetic effects.

61

62

63

64

65 Introduction

66
67 Sedimentary algal and bacterial pigments have been used for decades to gather
68 information about algal communities, aquatic productivity, eutrophication, redox (e.g.
69 meromixis), food web and light conditions, and water temperatures in lakes (Züllig 1982;
70 Lami et al. 2009; Bianchi and Canuel 2011). Sedimentary chlorophyll *a* (chl *a*) and
71 chlorophyll derivatives (pheopigments *a*, pheo *a*) are widely used as a proxy for past
72 phytoplankton biomass production (Bianchi and Canuel 2011; McGowan 2013).
73 Information about paleoproduction is important to understand the magnitude and
74 variability of natural and anthropogenic eutrophication, nutrient cycling and
75 temperature changes in aquatic systems through time (Belle et al. 2018).

76 Chloropigments (chls, the sum of chl and pheo) are labile molecules and a variety
77 of transformation products, such as pheophytin *a*, pyropheophytin *a*, pyropheophorbide
78 *a*, pheophorbide *a*, are readily formed during chemical and biological processes in lakes
79 including cellular senescence, photo oxidation and microbial oxidation, herbivore
80 grazing, among others (Leavitt 1993; Bianchi and Canuel 2011). Most chloropigments in
81 the euphotic zone are degraded through photo oxidation and enzymatic degradation to
82 colorless compounds (Rutherford 1989; Brown et al. 1991; Nugent 1996; Buchaca and
83 Catalan 2008). Some specific pheopigments *a* have been used as indicators of
84 zooplankton grazing. For instance, pheophorbide *a* (phide *a*) was found in protozoan fecal
85 pellets (Bianchi and Canuel 2011) and pyropheophorbide *a* (pyrophide *a*) was found in
86 copepod fecal pellets (Bianchi and Canuel 2011).

87 Several authors used the ratios between chlorophylls and chlorophyll derivatives to
88 assess the degree of pigment degradation and organic matter freshness. Buchaca and
89 Catalan (2008), for instance, introduced the Chl *a* Preservation Index (CPI) (chl *a*/ $\{$ chl
90 *a*+pheopigments *a* $\}$), Deshpande et al. (2014) used the ratio chl *a*/pheophytin *a*, and
91 Schubert et al. (2005) established the Chlorin Index to assess organic matter freshness in
92 sediments.

93 Nowadays, the identification and quantification of sedimentary pigments is mostly
94 obtained through advanced analytical techniques such as high-performance liquid
95 chromatography (HPLC) and gas chromatography (GC). These techniques are highly
96 compound-specific but they require high levels of expertise, labor and costs. In
97 consequence, long-term (e.g. Holocene) reconstructions are limited by the temporal

1
2
3
4
5
6
7
8
9
10
11
12
13
14
15
16
17
18
19
20
21
22
23
24
25
26
27
28
29
30
31
32
33
34
35
36
37
38
39
40
41
42
43
44
45
46
47
48
49
50
51
52
53
54
55
56
57
58
59
60
61
62
63
64
65

98 resolution and number of samples that can be processed in a reasonable time. Multi-lake
99 studies are very rare (Schubert et al. 2005).

100 To overcome these limitations, several researchers have explored and developed
101 more inexpensive and rapid methods either to measure bulk chloropigments directly from
102 lake sediments using VIS-VNIR reflectance spectroscopy (Butz et al. 2015; Michelutti
103 and Smol 2016) or to quantify specific chloropigments in synthetic and natural matrices
104 using spectrophotometric measurements of sediment extracts (Wetzel 1970; Jeffrey and
105 Humphrey 1975; Lichtenthaler and Buschmann 2001; Ritchie 2008). These latter
106 approaches apply mostly empirical or theoretical linear equations (mono-di-trichroic
107 equations) to the bulk spectrophotometric absorption spectra to infer specific
108 chloropigment concentrations in extracts. However, these approaches tend to
109 overestimate the concentrations of the parent chloropigments (chl *a*, chl *b*) in the presence
110 of diagenetic compounds (Ritchie 2008). Acidification techniques were proposed to
111 correct for the inaccuracy of universal algorithms (Lichtenthaler 1987; Jeffrey et al.
112 1997). Despite this further correction, the estimated concentration still may be incorrect
113 because (i) chl needs to be completely converted to 100% pheopigments through
114 acidification (Jeffrey et al. 1997) and, (ii) the background absorption needs to remain
115 constant before and after the acidification, which is mostly not the case as acidification
116 leads to turbidity (Küpper et al. 2007).

117 Recently, a different method has been developed with the aim to deconstruct the
118 bulk absorption spectrum of extracted samples as a weighted sum of individual
119 components through spectral deconvolution (Naqvi et al. 2004; Küpper et al. 2007;
120 Thrane et al. 2015). This approach was applied for the first time on lake sediment cores
121 by Thrane et al. (2015), who were able to correctly infer total chloropigment
122 concentrations. However, as mentioned above, a more species-specific identification and
123 accurate quantification of chloropigments and their related pheopigments is needed to
124 better understand aquatic paleoproduction, green algae biomass and chloropigments
125 preservation.

126 In this study, we developed a new method to quantify important chloropigment
127 species in lake sediments from bulk UV-VIS spectrophotometer absorption spectra using
128 spectral deconvolution. Our specific study goals were to develop a fast and inexpensive
129 alternative to existing methods for the simultaneous quantification of (i) chl *a* (an
130 indicator of aquatic paleoproduction (Bianchi and Canuel 2011)), (ii) chl *b* (an indicator
131 of green algae biomass (Jeffrey et al. 1997)), and (iii) pheo *a*, which combined with chl-

132 *a* allows the calculation of the Chlorophyll Preservation Index (CPI, Buchaca and Catalan
133 2008) that is used to assess (early) diagenetic effects in surface sediments and pigment
134 preservation through time. We test and validate our method on standard solutions and on
135 lake sediment samples collected from a sediment core in the Ponte Tresa sub-basin of
136 Lake Lugano, Switzerland. This lake was chosen because its eutrophication history is
137 well documented (Schneider et al. 2018) and pigments are thought to be well preserved
138 in anoxic sediments (Reuss et al. 2005).

139

140 Study site

141

142 Lake Lugano, southern Switzerland (Fig. 1) is of fluvio-glacial tectonic origin. The Ponte
143 Tresa sub-basin has a surface area of 1.1 km², a volume of 0.03 km³, a maximum depth
144 of 51 m, and is currently eutrophic (Simona 2003). The Ponte Tresa basin receives most
145 of its water from Lake Lugano. The mean water residence time is 0.04 years and the Tresa
146 River is its only outflow (annual discharge of 0.75 km³; Simona 2003). The regional
147 climate is temperate (Köppen classification) and characterized by mild winters, and warm
148 and humid summers (Niessen 1987). The catchment area is highly industrialized and
149 populated in the lowlands and along the lake shores, whereas the rest of the watershed is
150 mostly covered by mixed deciduous forest.

151 Sediments deposited during the 20th century are varved (biochemical varves) and
152 anoxic (Züllig 1982). The sediment composition, core chronology and eutrophication
153 history is well documented in Schneider et al. (2018). A first increase in aquatic
154 productivity was observed after 1930 followed by its maximum around 1964 and 1990
155 when the lake was highly eutrophic. Afterwards, wastewater treatment was widely
156 implemented and the eutrophication process started to slowly decline but remained at
157 very high levels. Despite the restoration measurement aimed at improving environmental
158 water quality, episodes of very high production with algal blooms were still observed in
159 the last decade due to internal nutrient cycling of the lake (Schneider et al. 2018; Tu et al.
160 2019).

161

162 **Materials and Methods**

163

164 Sediment sampling

165

166 We collected a short sediment core (PTRE 17-5-A) with an UWITEC gravity corer from
167 the deepest zone of the Ponte Tresa basin (45°58'02"N; 8°52'00"E, coring site in Fig. 1b)
168 in September 2017. After collection, the core was stored at 4 °C in a dark room. The core
169 was then split lengthwise and stratigraphically correlated with the dated core (PTRE-15-
170 3-A, Electronic Supplementary Material, ESM1) described in Schneider et al. (2018). For
171 the pigment analysis, 25 subsamples were taken at 2-cm contiguous intervals (sample
172 resolution about 4 years) back to an age of 1914.

173

174 Standard solution preparation

175

176 In this article we use the pigment terminology according to Bianchi and Canuel (2011)
177 and pigment abbreviations according to Welschmeyer (1994) and Jeffrey et al. (1997).

178 We prepared seven standard solutions with different concentrations of chl *a* and chl
179 *b*. Two solutions consisted of pure substances (chl *a* and chl *b*, respectively) whereas the
180 other five solutions contained concentration ratios (chl *a*/chl *b*) that range from 3.41 to
181 0.16 (Routh et al. 2009; Ramanathan et al. 2012; Waters et al. 2013; Mikomägi et al.
182 2016; Makri et al. 2019). In the standard solutions, the concentration of chl *a* and chl *b*
183 spanned from 1.20 to 6.10 mg L⁻¹ and from 1.79 to 7.53 mg L⁻¹, respectively.

184 We also prepared four standard solutions with chl *a* and pyropheophorbide *a* (i.e.,
185 a derivative of chl *a*). The concentrations of chl *a* spanned from 1.81 to 5.37 mg L⁻¹,
186 whereas that of pyropheophorbide *a* spanned from 2.41 to 8.78 mg L⁻¹. Concentration
187 ratios varied from 2.34 to 0.21 (chl *a*/pyropheophorbide *a*). Typical values for chl
188 *a*/pheopigments *a* found in eutrophic and oligotrophic lakes range between 2.5 and 0.5
189 (Guilizzoni et al. 1992; Dreßler et al. 2007; Makri et al. 2019).

190

191 Extraction and measurement methods for sedimentary pigments

192

193 The samples were extracted with a method modified from Reuss et al. (2005) with acetone
194 95%. For further details we refer to ESM2.

195 Chloropigments were analyzed with a UV-VIS spectrophotometer (Shimadzu, UV-
196 1800 CE, 230 V, 300-900 nm) at 0.1 nm step size and with a spectral bandwidth of 1 nm.
197 A Plastic UV-Cuvette micro with 1 cm of optical path (Brand GmbH & Co. KG,
198 Wertheim, Germany) was used. We optimized the z height center by having a total of 400
199 µL of solvent in the cuvette. The absorbance interval used for chloropigments

1
2
3
4
5
6
7
8
9
10
11
12
13
14
15
16
17
18
19
20
21
22
23
24
25
26
27
28
29
30
31
32
33
34
35
36
37
38
39
40
41
42
43
44
45
46
47
48
49
50
51
52
53
54
55
56
57
58
59
60
61
62
63
64
65

200 quantification spanned from 0.25 to 0.9 units. We selected this range because the
201 instrumental response is linearly correlated to concentration, more sensitive and less
202 prone to errors when constrained to this range (Lichtenthaler and Buschmann 2001).

203 Chloropigment species were analyzed by reversed-phase HPLC modified after
204 Lami et al. (2009), using an Agilent Infinity 1260 series equipped with a G7117C Diode-
205 Array Detection (DAD) detector and a G7121A fluorescence detector (FLD). A solution
206 composed of 25 μ L extracted sample in Acetone 100% HPLC grade was injected into an
207 Agilent Technologies column Omnisphere (250 mm x 4.6 mm, 5 μ m, Agilent
208 Technologies, Switzerland) through an Omnisphere replacement guard column (10 mm
209 x 3 mm, ChromGuard, Switzerland). The separation was carried out at 25 $^{\circ}$ C with a
210 solvent gradient as displayed in ESM3. Chloropigments species were identified and
211 quantified with standard compounds (ESM4), setting the DAD detector at different
212 wavelength of absorption (i.e., 432 nm for chl *a*, 468 nm for chl *b* and 408 nm for
213 pheopigments *a* to increase sensitivity). Furthermore, the FLD detector was set at $\lambda_{\text{ex}} =$
214 408 nm and $\lambda_{\text{emi}} = 668$ nm, and at $\lambda_{\text{ex}} = 432$ nm and $\lambda_{\text{emi}} = 668$ nm to double check the
215 correct identification of pheopigments *a* and chl *a*.

216 217 Peak deconvolution of UV-VIS bulk absorption spectra

218
219 In order to make the spectrophotometer measurements more compound specific and
220 accurate, we developed a new approach consisting of two consecutive steps:

221 Step 1: The spectrophotometric bulk absorption spectrum of sediment extracts (e.g.
222 red line in Fig. 2) is deconvoluted with an iterative non-linear least square (INLLS) fitting
223 (Küpper et al. 2007; O'Haver 2016) into a number of individual peaks (e.g. five peaks in
224 Fig. 2, for illustrative purposes). Those two peaks (orange and green in Fig. 2) that match
225 with their absorption maxima chls *a* and chls *b* are “targeted peaks” whereas the other
226 three peaks (gray lines in Fig. 2) are related to unknown substances or physical artifacts
227 (“untargeted peaks”). Step 1 serves to quantify the two components chls *a* and chls *b* from
228 the bulk spectrum.

229 Step 2: Dichroic equations are applied to one of the targeted peaks after Step 1 (e.g.
230 chloropigments *a* in Fig. 2) to separate chlorophyll (e.g. chl *a*) from the chlorophyll
231 derivatives (e.g. pheopigments *a*). This step serves to calculate the chlorophyll
232 preservation index (CPI).

233 In the following, further details about the two steps of our methodology are
234 provided.

235 Step 1: The bulk absorption spectrum, $X(\lambda)$ (abs), of a solution as a function of the
236 wavelength λ can be represented by a linear combination of J absorption spectra, $F_j(\lambda)$
237 (abs):

$$238 \quad X(\lambda) = \sum_{j=1}^J a_j F_j(\lambda) \quad (1)$$

239 where a_j are the weights defining the contribution of each j^{th} component to the total
240 absorbance. Each j^{th} absorption spectrum can be described with symmetrical or
241 asymmetrical functions, $F_j(\lambda, \delta_j, \omega_j)$, with the peak located at wavelength δ (nm) and the
242 half-width equal to ω (nm).

243 In order to obtain each j^{th} component of the bulk absorption spectrum, we used the
244 INLLS method (Küpper et al. 2007; O'Haver 2016). The INLLS method fits iteratively
245 the original spectrum, $X(\lambda)$, until the unknown model parameters (i.e., a_j , δ_j and ω_j) are
246 adjusted to minimize the sum-of-squared differences between the observed
247 spectrophotometer, $X_{\text{obs}}(\lambda)$, and the calculated absorbance, $X_{\text{cal}}(\lambda)$, from the INLLS
248 method (O'Haver 2016):

$$249 \quad \varepsilon(\lambda) = X_{\text{obs}}(\lambda) - X_{\text{cal}}(\lambda) \quad (2)$$

250 We tested seven symmetrical and six asymmetrical functions for describing $F_j(\lambda)$
251 (ESM5), and found that the Gaussian/Lorentzian blend function performed best compared
252 with the target pigments (highest R^2 , smallest root-mean-square deviation RMSD,
253 ESM6). The INLLS method was performed with a freely available peakFit algorithm
254 from the SPECTRUM package (O'Haver 2018) run in MatLab. As input model
255 parameters, we restricted the spectral interval of deconvolution to the range between 550
256 and 725 nm to avoid interference with carotenoids. Furthermore, we defined the number
257 of peaks per bulk spectrum (4 for standard solutions and 5 for sediment samples), the
258 number of iterations (100) and the instrumental noise (sample standard deviation
259 measured on 10 blank solutions). Tests have shown that a higher number of peaks per
260 bulk spectrum did not improve the results in our samples. The position, width and height
261 of the spectral peaks were not defined, and a baseline correction was not imposed. The
262 concentration c (mg L^{-1}) of chl b and chl a in standard solutions and chloropigments a in
263 sediment samples are quantified with the Beer-Lambert's law:

$$264 \quad c = A_\lambda / (\alpha_\lambda \cdot b) \quad (3)$$

265 where A_λ (abs) is the maximum absorbance at a given λ ; α_λ ($\text{L cm}^{-1} \text{mg}^{-1}$) is the absorbance
266 coefficient and b is the optical path which, in our case, is 1 cm. In standard solutions, the
267 absorbance coefficient is equal to $\alpha_{645.0} = 51.7 \cdot 10^{-3} \text{ L cm}^{-1} \text{mg}^{-1}$ for chl b (Lichtenthaler
268 1987) and $\alpha_{662.7} = 88.15 \cdot 10^{-3} \text{ L cm}^{-1} \text{mg}^{-1}$ for chl a (Jeffrey et al. 1997). In sediment
269 samples, chloropigments a are quantified using an absorbance coefficient of $a_{666} =$
270 $80.77 \cdot 10^{-3} \text{ L cm}^{-1} \text{mg}^{-1}$ (Jeffrey and Humphrey 1975).

271 Step 2: The concentrations of chl a and pyropheophorbide a in standard solutions
272 and chl a , and pheopigments a in sediment samples are quantified with the following
273 dichroic equations:

$$274 \quad C_{\text{Chl } a} = 57.81 \cdot A_{662.7} - 51.92 \cdot A_{666.0} \quad (4)$$

$$275 \quad C_{\text{Pheo } a/\text{Pyropheophorbide } a} = 63.08 \cdot A_{666.0} - 56.44 \cdot A_{662.7} \quad (5)$$

276 Both dichroic equations were developed after Lichtenthaler and Buschmann (2001)
277 in which we assume that pyropheophorbide a , pheophorbide a , pheophytin a and
278 pyropheophytin a have the same molar extinction coefficient of absorbance at 666.0 nm.
279 In our approach, these four diagenetic pigments in sediment samples are indistinguishable
280 and they are considered as the total pheopigments a .

281 We validate our method by (i) comparing the observed spectrophotometer $X_{\text{obs}}(\lambda)$
282 with the absorbance $X_{\text{cal}}(\lambda)$ as calculated from the INLLS method and, (ii) by comparing
283 the concentrations of the spectral deconvoluted peaks (SDPs) obtained from Eqs. 3-4-5
284 with the corresponding concentrations measured with the HPLC. We validate Step 1 with
285 the coefficients of determination (R^2) and root-mean-square deviation (RMSD) and Step
286 2 with the Adjusted Coefficient of Determination (R_{adj}^2) and root-mean-square error of
287 prediction (RMSEP). In Step 1 and 2 we used R^2 and R_{adj}^2 to estimate the match between
288 the experimental values and the values predicted by the deconvolution procedure. To
289 observe the correlation between two predicted variables the adjusted correlation
290 coefficient (r_{adj}) is used.

291

292 **Results**

293

294 Method validation with standard solutions

295

296 The observed $X_{\text{obs}}(\lambda)$ and fitted $X_{\text{cal}}(\lambda)$ bulk absorption spectra (Fig. 3a, blue and red lines)
297 are very similar showing RMSD values spanning from 0.4% to 0.8% (mean 0.6%).

1
2
3
4
5
6
7
8
9
10
11
12
13
14
15
16
17
18
19
20
21
22
23
24
25
26
27
28
29
30
31
32
33
34
35
36
37
38
39
40
41
42
43
44
45
46
47
48
49
50
51
52
53
54
55
56
57
58
59
60
61
62
63
64
65

298 Residual analyses between the observed and fitted bulk absorption spectra show that the
299 residuals are randomly distributed along the spectral range considered (550-725 nm) (Fig.
300 3b).

301 We observe that the deconvoluted peaks (targeted peaks) have their mean maxima
302 at $\lambda_{\max} = 662.38$ nm and $\lambda_{\max} = 645.90$ nm, which are typical values for chl *a* and chl *b*,
303 respectively (ESM7). Moreover, higher concentrations of chl *a* than chl *b* lead to red-shift
304 in the maximum absorption peak of the bulk spectrum (Fig. 3c). The opposite effect is
305 observed if chl *b* is more abundant than chl *a* (Fig. 3a). Residuals are randomly distributed
306 (Fig. 3b and d).

307 Fig. 4 shows the validation results of the deconvoluted spectral peaks for composite
308 standard solutions obtained from Eqs. 3-4-5 and the corresponding pigment
309 concentrations measured with the HPLC. In the standard solutions composed of chl *a* and
310 chl *b*, R_{adj}^2 spans between 0.98 and 0.99 (p-value $\sim 10^{-5}$, $n = 6$) with a RMSEP between
311 5% and 6 % (Fig. 4a-b). In standard mixtures of chl *a* and pyropheophorbide
312 *a*, R_{adj}^2 is 0.98 (p-value $\sim 10^{-3}$, $n = 4$) and RMSEP between 7% and 11% (Fig. 4c-d).
313 Residual analyses of the standard solutions show that the values are linearly independent
314 (scale-location plot), normally distributed (standardized residuals versus theoretical
315 quantiles and normal Q-Q plots), and no outliers are present based on the Cook's distance
316 (data not shown). The validation of the SDP results with the 'known' pigment
317 concentrations of the standard solutions yielded very similar results (ESM8).

318

319 Method validation on sediment samples

320

321 In contrast to standard solutions, extracts from environmental matrices (lake sediments)
322 contain many untargeted compounds that may interfere with the identification and
323 quantification of the target species. Therefore, we performed a validation with 25 samples
324 from a lake sediment core of the Ponte Tresa sub-basin, southern Swiss Alps. The
325 observed UV-VIS absorbance spectra (ESM9) and the fitted bulk absorption spectra show
326 a $R^2 > 0.9$ and RMSD between 0.2 % and 0.6 % with a mean value of 0.3 %. The validation
327 of the results from the spectral deconvolution (SDP obtained from Eqs. 3-4-5) with the
328 corresponding pigment concentrations as measured with the HPLC (chlorophyll *a*,
329 pyropheophorbide *a*, pheophorbide *a*, pheophytin *a* and pyropheophytin *a*) revealed R_{adj}^2
330 values for chloropigments *a*, chl *a* and pheopigments *a* ranging from 0.98 to 0.99 (p-
331 values $\leq 10^{-20}$) and RMSEP between 3% and 6% (Fig. 5a-c). The diagnostics of the linear

1
2
3
4
5
6
7
8
9
10
11
12
13
14
15
16
17
18
19
20
21
22
23
24
25
26
27
28
29
30
31
32
33
34
35
36
37
38
39
40
41
42
43
44
45
46
47
48
49
50
51
52
53
54
55
56
57
58
59
60
61
62
63
64
65

332 regression models for chloropigments *a*, chl *a* and pheopigments *a* show that the values
333 are linearly independent (scale-location plot and residual analysis), normally distributed
334 (standardized residuals versus theoretical quantiles and normal Q–Q plots) and no outliers
335 are present based on the Cook’s distance (ESM10, ESM11 and ESM12). In the case of
336 the Ponte Teresa sediment, the INLLS approach was not successful for the quantification
337 of chls *b* because the chls *a*/chls *b* ratio was very high (>10) and chls *b* concentrations
338 very low (< 10 µg g⁻¹).

340 Case study from the Ponte Tresa sub-basin (1914 – 2017)

341
342 In our case study, we focus on chlorophyll *a* and diagenetic products. The calculated SDP
343 concentrations of chloropigments *a*, pheopigments *a* and chl *a* agree with the HPLC
344 analyses along the entire sediment profile (Fig. 6a-c). We observe that the concentration
345 of these compounds increases over time (Fig. 6a): the oldest sediment (50 to 34 cm, ca.
346 1913 - 1952) is characterized by low chloropigment *a* concentrations (mean $c_{\text{chls } a, \text{SDP}} =$
347 $92 \mu\text{g g}_{\text{ds}}^{-1}$) and variability, which we attribute to relatively low primary production. At
348 a sediment depth between 34 and 24 cm (ca. 1952 - 1964), chloropigment *a* concentration
349 doubles (mean $c_{\text{chls } a, \text{SDP}} = 175 \mu\text{g g}_{\text{ds}}^{-1}$) with a local maximum at 34-32 cm (ca. 1952 -
350 1955; $c_{\text{chls } a, \text{SDP}} = 265 \mu\text{g g}_{\text{ds}}^{-1}$). The upper part of the sediment core from 24 to 0 cm (ca.
351 1964 - 2017) shows the highest chloropigments *a* concentrations (mean $c_{\text{chls } a, \text{SDP}} = 460$
352 $\mu\text{g g}_{\text{ds}}^{-1}$) and variability, associated with the highest paleoproduction. We observe three
353 relative chloropigments *a* maxima at 24-20 cm (ca. 1964 - 1973; $c_{\text{chls } a, \text{SDP}} = 503 \mu\text{g g}_{\text{ds}}^{-1}$),
354 at 14-10 cm (ca. 1987 - 1993; $c_{\text{chls } a, \text{SDP}} = 607 \mu\text{g g}_{\text{ds}}^{-1}$) and at 2-0 cm (ca. 2010 - 2017;
355 $c_{\text{chls } a, \text{SDP}} = 699 \mu\text{g g}_{\text{ds}}^{-1}$) (Fig. 6a).

356 HPLC data reveal that the degradation products of chl *a* are mostly composed of
357 pheophytin *a* >> pheophorbide *a* > pyropheophorbide *a* = pyropheophytin *a* (Fig. 6e).
358 The concentrations of pheophytin *a* show a marked increase in the 1950s and around
359 1968, 1988 and present day; pheophorbide *a* reveals a marked increase around 1988 (± 4
360 years) and in the last decade, whereas pyropheophorbide *a* and pyropheophytin *a* remain
361 at low levels and remarkably constant over time (Fig. 6e). Pheophytin *a* and chlorophyll
362 *a* are highly correlated with synchronous relative maxima. The proportion of
363 pheophorbide *a* relative to the other pheopigments increases above 22 cm sediment depth
364 (after ca. 1970).

1
2
3
4
5
6
7
8
9
10
11
12
13
14
15
16
17
18
19
20
21
22
23
24
25
26
27
28
29
30
31
32
33
34
35
36
37
38
39
40
41
42
43
44
45
46
47
48
49
50
51
52
53
54
55
56
57
58
59
60
61
62
63
64
65

365 The CPI values (chl *a*/{chl *a*+pheopigments *a*}; Buchaca and Catalan 2008)
366 calculated through "SDP-CPI" and "HPLC-CPI" approaches match well throughout the
367 sediment profile (Fig. 6d, $R^2_{\text{adj}} = 0.8$, p-value = 5.36×10^{-09} , n = 25). The CPI values vary
368 within a small range from 0.28. to 0.48 with a positive trend (p<0.01) toward the top of
369 the core. The CPI values do not show a 'tailing' (anomaly) in the topmost centimeters of
370 the sediment with smaller CPI values (less pigment degradation, 'fresher' sediment),
371 suggesting that there is no discernable early diagenetic pigment degradation in the
372 topmost sediment. The CPI values are weakly correlated with the total aquatic production
373 as indicated by chls *a* ($r_{\text{adj}} = 0.35$, p-value = 0.045, n = 25).

374 The ratios of chl *a* to three of the four pheopigments (pyropheophorbide *a*,
375 pheophorbide *a*, pyrophytin *a*) are >1.0 throughout the entire core (ESM13), whereas the
376 ratios of chl *a* to pheophytin-*a* are mostly <1.0 except for the topmost sediment and two
377 samples at the bottom of our sediment core. The correlation between the ratios chl
378 *a*/pyropheophytin *a* and the CPI ($r_{\text{adj}} = 0.81$, p-value = 10^{-16} , n = 25), chl *a*/pheophytin *a*
379 and CPI ($r_{\text{adj}} = 0.73$, p-value = 10^{-15} , n = 25), chl *a*/pyropheophorbide *a* and CPI ($r_{\text{adj}} =$
380 0.65, p-value = 10^{-15} , n = 25), and chl *a*/pheophorbide *a* and CPI ($r_{\text{adj}} = 0.35$, p-value =
381 10^{-13} , n = 25) are all statistically significant.

382

383 Discussion

384

385 The goal of this study was to develop a low-cost and rapid method to provide more
386 detailed information about chloropigments (parent and diagenetic compounds) and their
387 use as proxies for aquatic paleoproduction, green algae biomass (Bianchi and Canuel
388 2011) and chlorophylls preservation (Buchaca and Catalan 2008).

389 Compared with HPLC analysis, our approach provides less specific pigment
390 information, but it has the advantage to quantify chl *a*, pheopigments *a* and, potentially
391 chl *b* in sediment extracts at lower costs and less time (ca. 20 minutes measurement and
392 analysis time). The laboratory infrastructure and maintenance is cheaper and staff training
393 is easier. Although substantial development work is still required, the approach could
394 potentially be applied on bulk VIS-VNIR spectra (Butz et al. 2015; Michelutti and Smol
395 2016) that are obtained directly from sediments without prior pigment extraction. This
396 needs to be explored.

397 The method validation on standards showed that the INLLS method (Step 1),
398 followed by the application of mono-/dichroic equations (Step 2) allows us to infer chl *a*,

399 chl *b* (parent compounds) and derivatives (pheopigments-a) from bulk spectrophotometer
400 absorption spectra with typical RMSE of 7-11 %. In general, chls *b* detection and
401 quantification through INLLS is difficult in the presence of high chls *a* concentration
402 since the molar extinction coefficients of chls *b* are smaller than those of chls *a* in the
403 UV-VIS red range (Jeffrey et al. 1997). From our measurements of the standards it
404 appears that our method is able to accurately quantify chl *b* when the concentration ratio
405 of chl *a*/chl *b* is between 3.41 and 0.16. Higher or lower concentration ratios of chl *a*/chl
406 *b* have not been tested yet and need to be further explored. In our case study of Ponte
407 Tresa, the concentrations of chls *b* are very low ($< 10 \mu\text{g g}^{-1}$) and the ratio chls *a*/chls *b* is
408 high (>10 ; Schneider et al. 2018) which is likely the reason why our approach was not
409 successful to quantify chls *b*. According to the results from the standard solutions, the
410 quantification of chls *b* should be possible with our approach in sediments if the chls
411 *a*/chls *b* ratio is lower than 3.4.

412 Following Bianchi and Canuel (2011), we diagnose aquatic paleoproduction and,
413 ultimately, eutrophication through the quantification of chls *a*. In our case study of Ponte
414 Tresa (1913-2017, Fig. 6a-c), the eutrophication history as reconstructed by the SDP
415 method compares very well with both the data measured by HPLC and the eutrophication
416 history of Lake Lugano and the Ponte Tresa basin as reported in the literature (Züllig
417 1982; Barbieri et al. 1992; Polli and Simona 1992; Lotter 2001; Lepori and Roberts 2015;
418 Schneider et al. 2018). Oligotrophic/mesotrophic conditions prevailed at the beginning of
419 the 20th century, eutrophication started in the 1940-1950s, and highly eutrophic conditions
420 persisted from 1964 to the present.

421 Although it is well established that chlorophyll degradation occurs in the water
422 column and in sediments (Daley 1973; Carpenter et al. 1986; Hurley and Armstrong
423 1991), most of the literature focuses on the chlorophyll degradation in the water column
424 (Daley 1973; Leavitt and Brown 1988; Leavitt 1993). Post-burial pigment degradation,
425 particularly early diagenetic effects in the topmost sediments are still poorly understood.
426 For sedimentary organic matter, Gälman et al. (2008) reported post-burial losses of up to
427 20% for C and 30% for N within five years after deposition. Interpreting the CPI as a
428 proxy for pigment degradation in the water column relies on the assumption that post-
429 sedimentary pigment degradation and early diagenesis is limited, which is likely under
430 anoxic conditions and the absence of light and bioturbation (Bianchi and Canuel 2011).
431 In the sediment of the Ponte Tresa basin, the CPI values of the sediment of the past 100
432 years (Fig. 6d) do not show an exponential decline towards the sediment surface, as one

1
2
3
4
5
6
7
8
9
10
11
12
13
14
15
16
17
18
19
20
21
22
23
24
25
26
27
28
29
30
31
32
33
34
35
36
37
38
39
40
41
42
43
44
45
46
47
48
49
50
51
52
53
54
55
56
57
58
59
60
61
62
63
64
65

433 would expect from early diagenetic degradation of chlorophyll in the top sediments.
434 Similar results were also found in other eutrophic lakes (Deshpande et al. 2014; Makri et
435 al. 2019). The constant CPI values, particularly in the topmost 12 cm (Fig. 6d) suggest
436 that, in the deep Ponte Tresa sub-basin with mostly hypoxic conditions in the
437 hypolimnion, limited light transparency (Secchi depth mostly between 2 and 8 m; at Figino
438 station) and anoxic varved sediment (no bioturbation), early diagenetic transformation of
439 chloropigments is limited, and chloropigments species are well preserved. This is
440 different from well- oxygenated oligotrophic Alpine lakes where trends of chloropigment
441 ratios in the topmost sediments were observed (Guilizzoni et al. 1992).

442 443 **Conclusions**

444
445 The purpose of our study was to develop and evaluate the spectral deconvoluted peak
446 SDP approach in order to obtain more information about chloropigments from UV-VIS
447 bulk spectrophotometer absorption spectra of sediment extracts. We applied the approach
448 on sediment from a lake with a relatively well-known productivity history.

449 On standard solutions, our mathematical approach is able to quantify chlorophyll *a*
450 and chlorophyll *b* and pheopigments *a* from bulk UV-VIS absorption spectra. The method
451 validation on sediment extracts revealed a RMSE between 3-6%. Our approach serves to
452 obtain, in a cost-efficient and time-efficient way, more specific information about
453 sedimentary pigments, which is relevant to infer paleoproduction, Chlorophyll
454 Preservation Index and early diagenetic effects in surface sediments and, potentially,
455 green algae biomass.

456 In our case study from the Ponte Tresa basin covering the past 100 years, the
457 eutrophication history inferred from our method compares favorably with the
458 eutrophication history as inferred from HPLC measurements and reported in the
459 literature. The CPI values in the topmost sediment suggest that early diagenetic effects
460 are limited and pigments are relatively well preserved once they are buried in anoxic
461 sediments under low light conditions.

462 Our methodological approach is regarded as a first step towards inexpensive and
463 rapid assessments of sedimentary chlorophylls and their related pheopigments from bulk
464 UV-VIS spectra. In the future, this spectral deconvolution method could, potentially, be
465 applied on bulk UV-VIS spectra measured directly on sediment subsamples or maybe
466 even on entire half-cores.

467

1
2 **468 Acknowledgements**

3
4 **469**

5 470 This work was supported by the Swiss National Science Foundation (Grant
6
7 471 200021_172586). The authors thank Dr. Andrea Lami for his support with the HPLC
8
9 472 method and Dr. Daniela Fischer for laboratory assistance. We thank the two anonymous
10
11 473 reviewers and the Associate Editor for thoughtful comments and suggestions.

12
13 **474**

14 **475 Author contributions**

15
16 **476**

17
18 477 AS and MG designed the research. AS carried out the analytical and methodological
19
20 478 work, and AS and MG wrote the paper.

21
22 **479**

23 **480 Data Accessibility**

24
25 481 The data are stored at www.pangaea.de

26
27 **482**

28
29 **483 References**

30
31 **484**

32
33 485 Barbieri A, Mosello R (1992) Chemistry and trophic evolution of Lake Lugano in relation
34
35 486 to nutrient budget. *Aquat Sci* 54: 219-237. <https://doi.org/10.1007/BF00878138>

36 487 Belle S, Musazzi S, Lami A (2018) Glacier dynamics influenced carbon flows through
37
38 488 lake food webs: evidence from a chironomid $\delta^{13}\text{C}$ -based reconstruction in the
39
40 489 Nepalese Himalayas. *Hydrobiologia* 809: 285-295.
41
42 490 <https://doi.org/10.1007/s10750-017-3477-8>

43
44 491 Bianchi TS, Canuel EA (2011) Chemical biomarkers in aquatic ecosystems. Princeton
45
46 492 University Press, Princeton. <https://doi.org/10.1515/9781400839100>

47 493 Brown SB, Houghton JD, Hendry GAF (1991) Chlorophyll breakdown. In: H. Scheer,
48
49 494 (ed) *Chlorophylls*. CRC Press, Boca Raton, pp 465-489.

50
51 495 Buchaca T, Catalan J (2008) On the contribution of phytoplankton and benthic biofilms
52
53 496 to the sediment record of marker pigments in high mountain lakes. *J Paleolimnol*
54
55 497 40: 369-383. <https://doi.org/10.1007/s10933-007-9167-1>

56 498 Butz C, Grosjean M, Fischer D, Wunderle S, Tylmann W, Rein B (2015) Hyperspectral
57
58 499 imaging spectroscopy: a promising method for the biogeochemical analysis of

60
61
62
63
64
65

1 lake sediments. *Journal of Applied Remote Sensing* 9: 096031.
2 <https://doi.org/10.1117/1.JRS.9.096031>

3
4 502 Carpenter SR, Elser MM, Elser JJ (1986) Chlorophyll production, degradation, and
5 503 sedimentation: Implications for paleolimnology. *Limnol Oceanogr* 31: 112-124.
6 <https://doi.org/10.4319/lo.1986.31.1.0112>

7
8 504 Daley RJ, Brown SR (1973) Experimental characterization of lacustrine chlorophyll
9 505 diagenesis. I. Physiological and environmental effects. *Arch Hydrobiol* 72: 277-
10 506 304.

11
12 507
13
14 508 Deshpande BN, Tremblay R, Pienitz R, Vincent WF (2014) Sedimentary pigments as
15 509 indicators of cyanobacterial dynamics in a hypereutrophic lake. *J Paleolimnol* 52:
16 510 171-184. <https://doi.org/10.1007/s10933-014-9785-3>

17
18 511 Dreßler M, Hübener T, Görs S, Werner P, Selig U (2007) Multi-proxy reconstruction of
19 512 trophic state, hypolimnetic anoxia and phototrophic sulphur bacteria abundance
20 513 in a dimictic lake in Northern Germany over the past 80 years. *J Paleolimnol* 37:
21 514 205-219. <https://doi.org/10.1007/s10933-006-9013-x>

22
23 515 Gälman V, Rydberg J, de- Luna SS, Bindler R, Renberg I (2008) Carbon and nitrogen
24 516 loss rates during aging of lake sediment: changes over 27 years studied in varved
25 517 lake sediment. *Limnol Oceanogr* 53: 1076-1082.
26 518 <https://doi.org/10.4319/lo.2008.53.3.1076>

27
28 519 Guilizzoni P, Lami A, Marchetto A (1992) Plant pigment ratios from lakes sediments as
29 520 indicators of recent acidification in alpine lakes. *Limnol Oceanogr* 37: 1565-1569.
30 521 <https://doi.org/10.4319/lo.1992.37.7.1565>

31
32 522 Hurley JP, Armstrong DE (1991) Pigment preservation in lake sediments: a comparison
33 523 of sedimentary environments in Trout Lake, Wisconsin. *Can J Fish Aquat Sci* 48:
34 524 472-486. <https://doi.org/10.1139/f91-061>

35
36 525 Jeffrey ST, Humphrey GF (1975) New spectrophotometric equations for determining
37 526 chlorophylls a, b, c1 and c2 in higher plants, algae and natural phytoplankton.
38 527 *Biochemie und Physiologie der Pflanzen* 167: 191-194.
39 528 [https://doi.org/10.1016/S0015-3796\(17\)30778-3](https://doi.org/10.1016/S0015-3796(17)30778-3)

40
41 529 Jeffrey SW, Mantoura RFC, Wright SW (1997) Phytoplankton pigments in
42 530 oceanography. UNESCO, Paris. <https://doi.org/10.1017/S0025315400036389>

43
44 531 Küpper H, Seibert S, Parameswaran A (2007) Fast, sensitive, and inexpensive alternative
45 532 to analytical pigment HPLC: quantification of chlorophylls and carotenoids in
46
47
48
49
50
51
52
53
54
55
56
57
58
59
60
61
62
63
64
65

533 crude extracts by fitting with Gauss peak spectra. *Anal Chem* 79: 7611-7627.
534 <https://doi.org/10.1021/ac070236m>

535 Lami A, Musazzi S, Marchetto A, Buchaca T, Kernan M, Jeppesen E, Guilizzoni P (2009)
536 Sedimentary pigments in 308 alpine lakes and their relation to environmental
537 gradients. *Adv Limnology* 62: 247-268.

538 Leavitt PR, Brown SR (1988) Effects of grazing by *Daphnia* on algal carotenoids:
539 Implications for paleolimnology. *J Paleolimnol* 1: 201-213.
540 <https://doi.org/10.1007/BF00177766>

541 Leavitt PR (1993) A review of factors that regulate carotenoid and chlorophyll deposition
542 and fossil pigment abundance. *J Paleolimnol* 9: 109-127.
543 <https://doi.org/10.1007/BF00677513>

544 Lepori F, Roberts JJ (2015) Past and future warming of a deep European lake (Lake
545 Lugano): What are the climatic drivers? *J Great Lakes Res* 41: 973-981.
546 <https://doi.org/10.1016/j.jglr.2015.08.004>

547 Lichtenthaler HK (1987) Chlorophylls and carotenoids: pigments of photosynthetic
548 biomembranes. *Meth. Enzymol* 148: 350–382. [https://doi.org/10.1016/0076-
549 6879\(87\)48036-1](https://doi.org/10.1016/0076-6879(87)48036-1)

550 Lichtenthaler HK, Buschmann C (2001) Chlorophylls and carotenoids: Measurement and
551 characterization by UV- VIS spectroscopy. *Current protocols in food analytical
552 chemistry* 1: F4.3.1-F4.3.8. <https://doi.org/10.1002/0471142913.faf0403s01>

553 Lotter AF (2001) The effect of eutrophication on diatom diversity: examples from six
554 Swiss lakes. In: Jahn R, Kociolek JP, Witkowski A, Compère P (eds) *Studies on
555 diatoms*. Ganter, Ruggell, pp 417–432.

556 Makri S, Lami A, Lods-Crozet B, Loizeau JL (2019) Reconstruction of trophic state shifts
557 over the past 90 years in a eutrophicated lake in western Switzerland, inferred
558 from the sedimentary record of photosynthetic pigments. *J Paleolimnol* 61: 129-
559 145. <https://doi.org/10.1007/s10933-018-0049-5>

560 McGowan S (2013) Pigment studies. In: Elias S., Mock C.J. (eds): *Encyclopedia of
561 Quaternary Sciences*. Elsevier, Amsterdam, pp 326–338.
562 <https://doi.org/10.1016/B978-0-444-53643-3.00235-1>

563 Michelutti N, Smol JP (2016) Visible spectroscopy reliably tracks trends in paleo-
564 production. *J Paleolimnol* 56: 253-265. [https://doi.org/10.1007/s10933-016-9921-
565 3](https://doi.org/10.1007/s10933-016-9921-3)

- 1
2
3
4
5
6
7
8
9
10
11
12
13
14
15
16
17
18
19
20
21
22
23
24
25
26
27
28
29
30
31
32
33
34
35
36
37
38
39
40
41
42
43
44
45
46
47
48
49
50
51
52
53
54
55
56
57
58
59
60
61
62
63
64
65
- 566 Mikomägi A, Koff T, Martma T, Marzecová A (2016) Biological and geochemical
567 records of human-induced eutrophication in a small hard-water lake. *Boreal*
568 *Environ Res* 21: 513-527.
- 569 Naqvi KR, Hassan TH, Naqvi YA (2004) Expeditious implementation of two new
570 methods for analysing the pigment composition of photosynthetic specimens.
571 *Spectrochim Acta Part A Mol Biomol Spectrosc* 60: 2783-2791.
572 <https://doi.org/10.1016/j.saa.2004.01.017>
- 573 Niessen F (1987) *Sedimentologische, geophysikalische und geochemische*
574 *Untersuchungen zur Entstehung und Ablagerungsgeschichte des Luganersees*
575 *(Schweiz)*. (Doctoral dissertation, ETH Zurich).
- 576 Nugent JH (1996) Oxygenic photosynthesis: electron transfer in photosystem I and
577 photosystem II. *Eur J Biochem* 237(3): 519-531. [https://doi.org/10.1111/j.1432-](https://doi.org/10.1111/j.1432-1033.1996.00519.x)
578 [1033.1996.00519.x](https://doi.org/10.1111/j.1432-1033.1996.00519.x)
- 579 O'Haver T (2016) *A Pragmatic Introduction to Signal Processing*. Lulu Enterprises
580 Incorporated.
- 581 O'Haver T (2018) Toolkit of functions, scripts and spreadsheet templates.
582 <https://terpconnect.umd.edu/~toh/spectrum/peakfit.m> Accessed 30 March 2019.
- 583 Polli B, Simona M (1992) Qualitative and quantitative aspects of the evolution of the
584 planktonic populations in Lake Lugano. *Aquat Sci* 54: 303-320.
585 <https://doi.org/10.1007/BF00878143>
- 586 Ramanathan A, Datta DK, Ghosh P, Kaushal S, Murtugudde R (2012) Tracing Nitrogen
587 and Carbon Biogeochemical Processes in the Inter-tidal Mangrove Ecosystem
588 (Sundarban) of India and Bangladesh: Implications of the Global Environmental
589 Change. Asia-Pacific Network for Global Change Research. [http://www.apn-](http://www.apn-gcr.org/resources/index.php/items/show/1598)
590 [gcr.org/resources/index.php/items/show/1598](http://www.apn-gcr.org/resources/index.php/items/show/1598)
- 591 Reuss N, Conley DJ (2005) Effects of sediment storage conditions on pigment analyses.
592 *Limnol Oceanogr* 3: 477-487. <https://doi.org/10.4319/lom.2005.3.477>
- 593 Ritchie RJ (2008) Universal chlorophyll equations for estimating chlorophylls a, b, c, and
594 d and total chlorophylls in natural assemblages of photosynthetic organisms using
595 acetone, methanol, or ethanol solvents. *Photosynthetica* 46: 115-126.
596 <https://doi.org/10.1007/s11099-008-0019-7>
- 597 Routh J, Choudhary P, Meyers PA, Kumar B (2009) A sediment record of recent nutrient
598 loading and trophic state change in Lake Norrviken, Sweden. *J Paleolimnol* 42:
599 325-341. <https://doi.org/10.1007/s10933-008-9279-2>.

- 1
2
3
4
5
6
7
8
9
10
11
12
13
14
15
16
17
18
19
20
21
22
23
24
25
26
27
28
29
30
31
32
33
34
35
36
37
38
39
40
41
42
43
44
45
46
47
48
49
50
51
52
53
54
55
56
57
58
59
60
61
62
63
64
65
- 600 Rutherford AW (1989) Photosystem II, the water-splitting enzyme. *Trends Biochem Sci*
601 14: 227-232. [https://doi.org/10.1016/0968-0004\(89\)90032-7](https://doi.org/10.1016/0968-0004(89)90032-7)
- 602 Schneider T, Rimer D, Butz C, Grosjean M (2018) A high-resolution pigment and
603 productivity record from the varved Ponte Tresa basin (Lake Lugano,
604 Switzerland) since 1919: insight from an approach that combines hyperspectral
605 imaging and high-performance liquid chromatography. *J Paleolimnol* 60: 381-
606 398. <https://doi.org/10.1007/s10933-018-0028-x>
- 607 Schubert CJ, Niggemann J, Klockgether G, Ferdelman TG (2005) Chlorin index: a new
608 parameter for organic matter freshness in sediments. *Geochemistry, Geophysics,*
609 *Geosystems* 6. <https://doi.org/10.1029/2004GC000837>
- 610 Simona M (2003) Winter and spring mixing depths affect the trophic status and
611 composition of phytoplankton in the northern meromictic basin of Lake Lugano.
612 *J Limnol* 62: 190-206. <https://doi.org/10.4081/jlimnol.2003.190>
- 613 Thrane JE, Kyle M, Striebel M, Haande S, Grung M, Rohrlack T, Andersen T (2015)
614 Spectrophotometric analysis of pigments: a critical assessment of a high-
615 throughput method for analysis of algal pigment mixtures by spectral
616 deconvolution. *PloS one*, 10(9): e0137645.
617 <https://doi.org/10.1371/journal.pone.0137645>
- 618 Tu L, Jarosch K, Schneider T, Grosjean M (2019) Phosphorus fractions in sediments and
619 their relevance for historical lake eutrophication in the Ponte Tresa basin (Lake
620 Lugano, Switzerland) since 1959. *Science of The Total Environment* 685: 806-
621 817. <https://doi.org/10.1016/j.scitotenv.2019.06.243>
- 622 Waters MN, Smoak JM, Saunders CJ (2013) Historic primary producer communities
623 linked to water quality and hydrologic changes in the northern Everglades. *J*
624 *Paleolimnol* 49: 67-81. <https://doi.org/10.1007/s10933-011-9569-y>
- 625 Welschmeyer NA (1994) Fluorometric analysis of chlorophyll a in the presence of
626 chlorophyll b and pheopigments. *Limnol Oceanogr* 39: 1985-1992.
627 <https://doi.org/10.4319/lo.1994.39.8.1985>
- 628 Wetzel RG (1970) Recent and postglacial production rates of a marl lake. *Limnol*
629 *Oceanogr* 15: 491-503. <https://doi.org/10.4319/lo.1970.15.4.0491>
- 630 Züllig H (1982) Untersuchungen über die Stratigraphie von Carotinoiden im
631 geschichteten Sediment von 10 Schweizer Seen zur Erkundung früherer
632 Phytoplankton-entfaltungen. *Schweizerische Zeitschrift für Hydrologie* 44: 1-98.
633 <https://doi.org/10.1007/BF02502191>

634

- 1
- 2
- 3
- 4
- 5
- 6
- 7
- 8
- 9
- 10
- 11
- 12
- 13
- 14
- 15
- 16
- 17
- 18
- 19
- 20
- 21
- 22
- 23
- 24
- 25
- 26
- 27
- 28
- 29
- 30
- 31
- 32
- 33
- 34
- 35
- 36
- 37
- 38
- 39
- 40
- 41
- 42
- 43
- 44
- 45
- 46
- 47
- 48
- 49
- 50
- 51
- 52
- 53
- 54
- 55
- 56
- 57
- 58
- 59
- 60
- 61
- 62
- 63
- 64
- 65

635

636 **Figure captions**

637 **Fig. 1** a) Location of Lake Lugano within Switzerland and the Ponte Tresa sub-basin (red
638 rectangle). b) Bathymetric map of Ponte Tresa sub-basin. The black asterisk marks the
639 coring site (figure from Schneider et al. 2018).

640 **Fig. 2** The bulk UV-VIS spectrum (red line) of a sediment extract of unknown
641 composition is deconvoluted into five peaks using an iterative non-linear least square
642 fitting: the orange and green peaks are characteristic for chloropigments *b* (chls *b*, green
643 algae) and chloropigments *a* (chls *a*, mainly aquatic paleoproduction) whereas the other
644 three peaks (grey lines) represent unknown (non-chlorophyll *a* or *b*) substances or
645 physical artifacts. This sample is for illustrative purposes (i.e. a sediment sample from
646 Ponte Tresa spiked with chl *b*).

647 **Fig. 3** (a, c): Observed UV-VIS bulk spectrum, $X_{obs}(\lambda)$ (blue), fitted spectra, $X_{cal}(\lambda)$
648 (red), deconvoluted spectra for chl *a* (green), chl *b* (orange), and for two unknown (non-
649 chlorophyll *a* or *b*) substances or physical artifacts (grey); (b, d) residuals (pink dots),
650 $X_{obs}(\lambda) - X_{cal}(\lambda)$. The results are reported for a standard solution in which chl *b* \gg chl *a*
651 (Fig. 3a) and chl *a* \gg chl *b* (Fig. 3c).

652 **Fig. 4** Method validation between HPLC measured and SDP calculated concentrations
653 for (a-b) seven standard solutions with mixtures of chl *a* and chl *b* and (c-d) four
654 standard solutions with mixtures of chl *a* and pyropheorbide *a*. The black dashed lines
655 delimit the 95% confidence interval for the regression function (red) and the green lines
656 indicate the range of the predicted values (green).

657 **Fig. 5** Method validation between HPLC measured and SDP calculated concentrations
658 for (a) chloropigments *a*, (b) pheopigments *a* and (c) chl *a* in sediment samples of the
659 Ponte Tresa sub-basin of Lake Lugano. The black dashed lines delimit the 95%
660 confidence intervals for the regression function (red) and the green lines indicate the
661 range of the predicted values (green).

662 **Fig. 6** Pigment stratigraphy of the sediment core PTRE 17-5 (Ponte Tresa sub-basin)
663 showing the comparison between HPLC-measured and SDP-calculated concentrations
664 for a) chloropigments *a* (chls *a*); b) pheopigments (p heo *a*; c) chl *a*, d) CPI and, e)
665 specific pheopigments *a*: pyropheophorbide *a* (pyrophide *a*), pheophorbide *a* (phide *a*),
666 pheophytin *a* (phytin *a*) and pyrophephytin *a* (pyrophytin *a*) obtained through HPLC.
667 The green colors show the Ponte Tresa trophic state according to Schneider et al.
668 (2018).

669

670

671

672

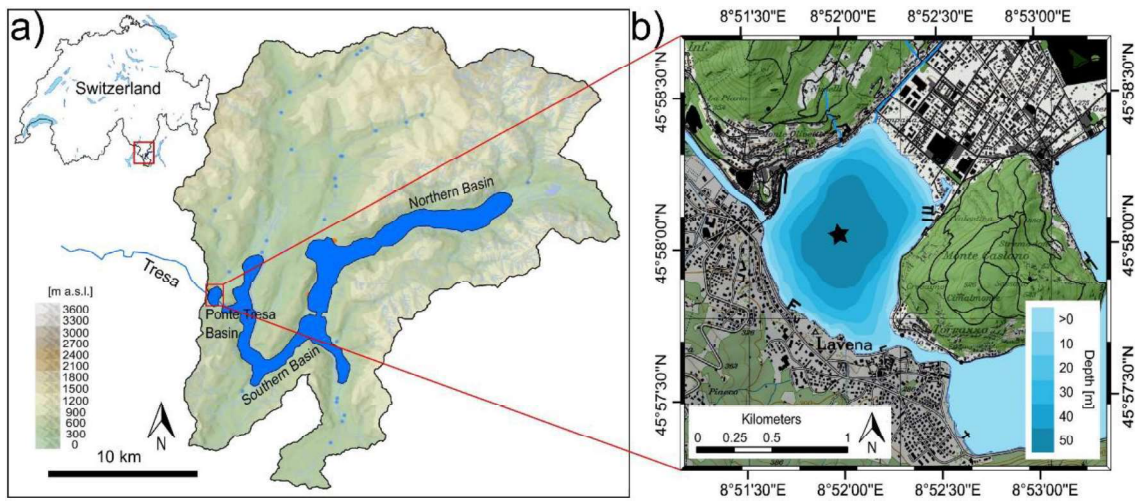
673

674

675

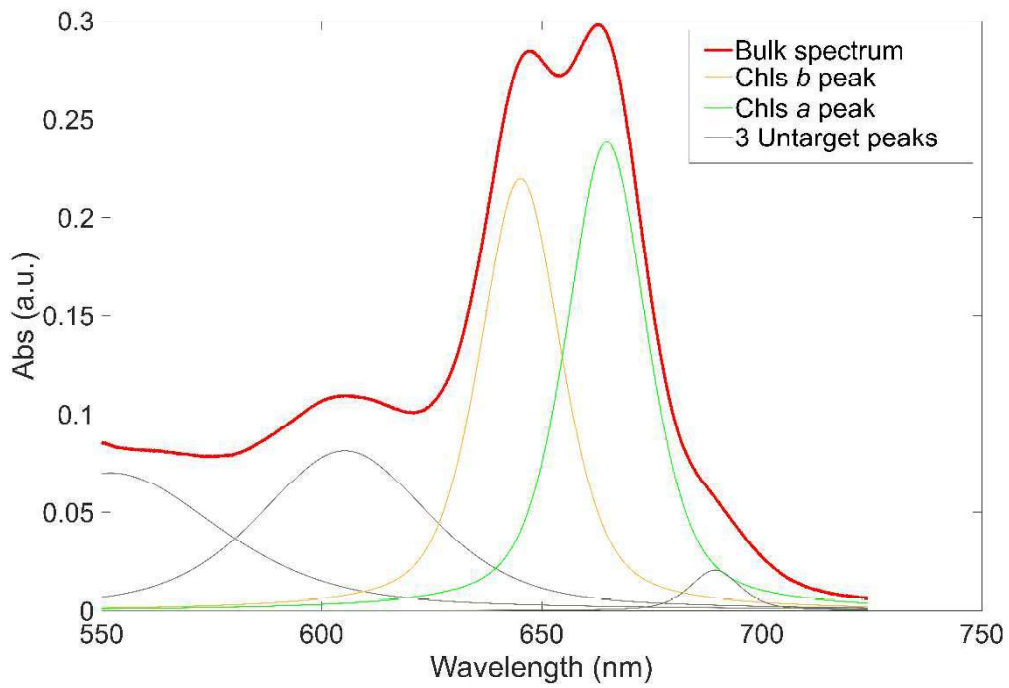
1
2
3
4
5
6
7
8
9
10
11
12
13
14
15
16
17
18
19
20
21
22
23
24
25
26
27
28
29
30
31
32
33
34
35
36
37
38
39
40
41
42
43
44
45
46
47
48
49
50
51
52
53
54
55
56
57
58
59
60
61
62
63
64
65

676 **Figures**



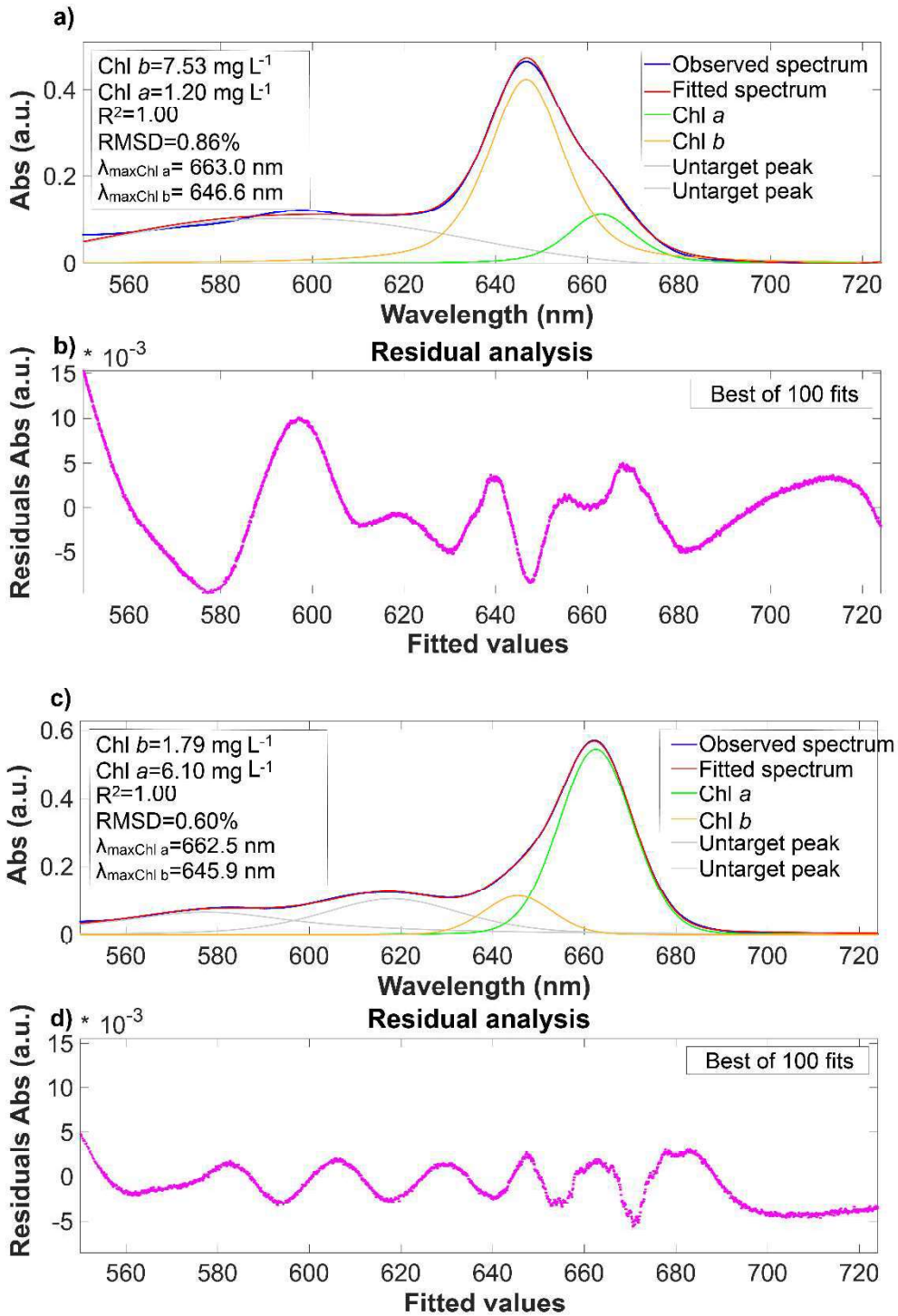
677

678 **Fig. 1**



679

680 **Fig.2**

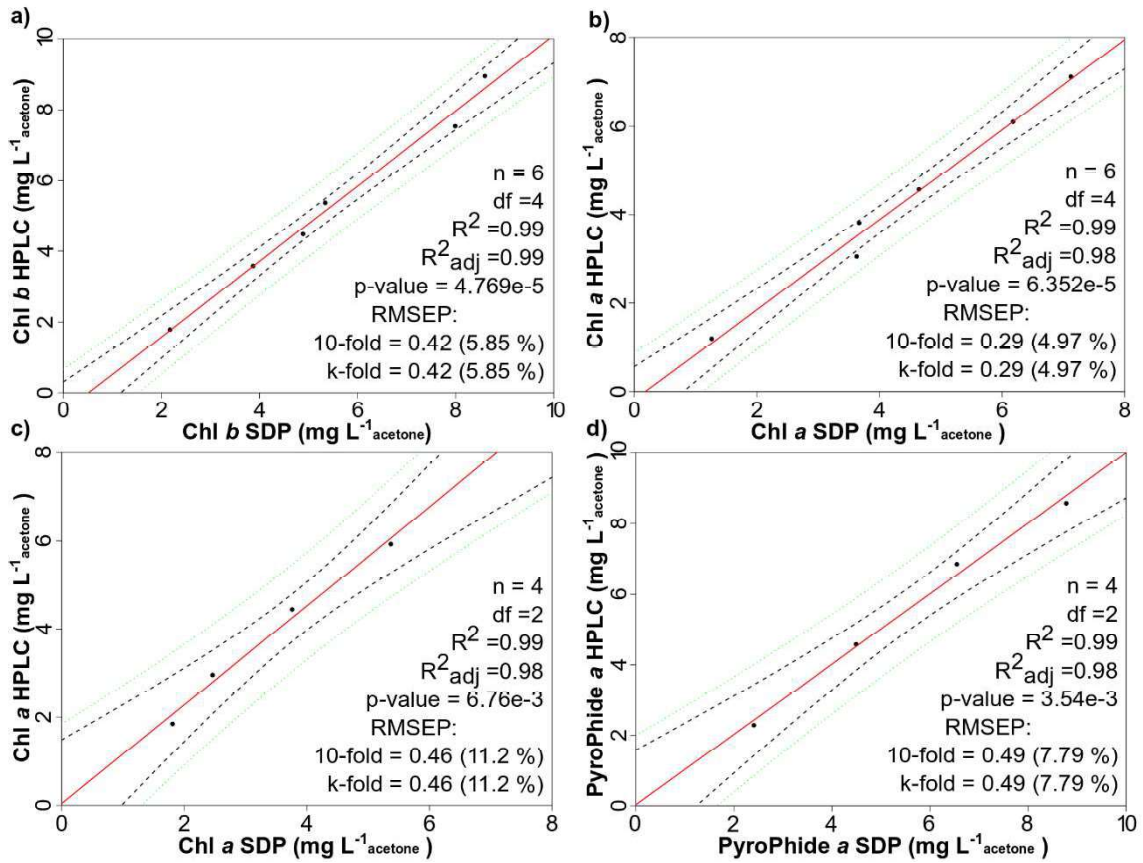


681

682

Fig.3

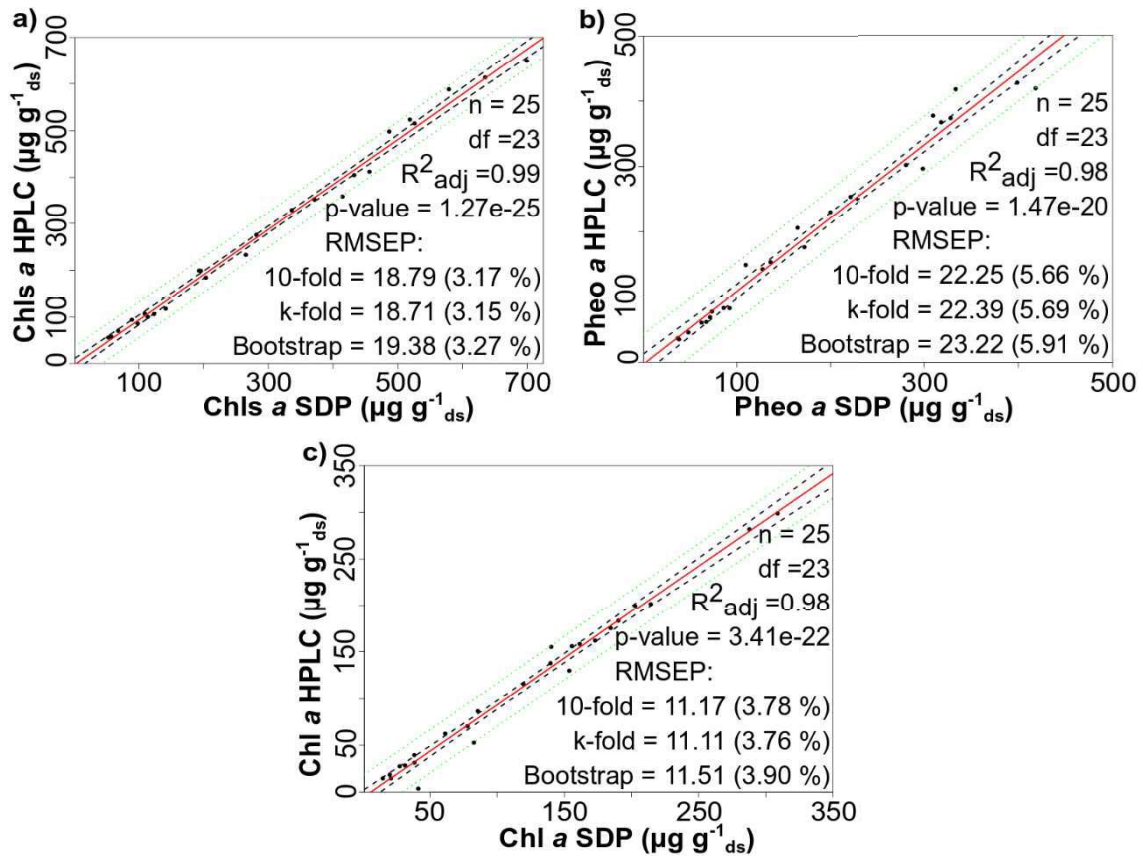
1
2
3
4
5
6
7
8
9
10
11
12
13
14
15
16
17
18
19
20
21
22
23
24
25
26
27
28
29
30
31
32
33
34
35
36
37
38
39
40
41
42
43
44
45
46
47
48
49
50
51
52
53
54
55
56
57
58
59
60
61
62
63
64
65



683

684

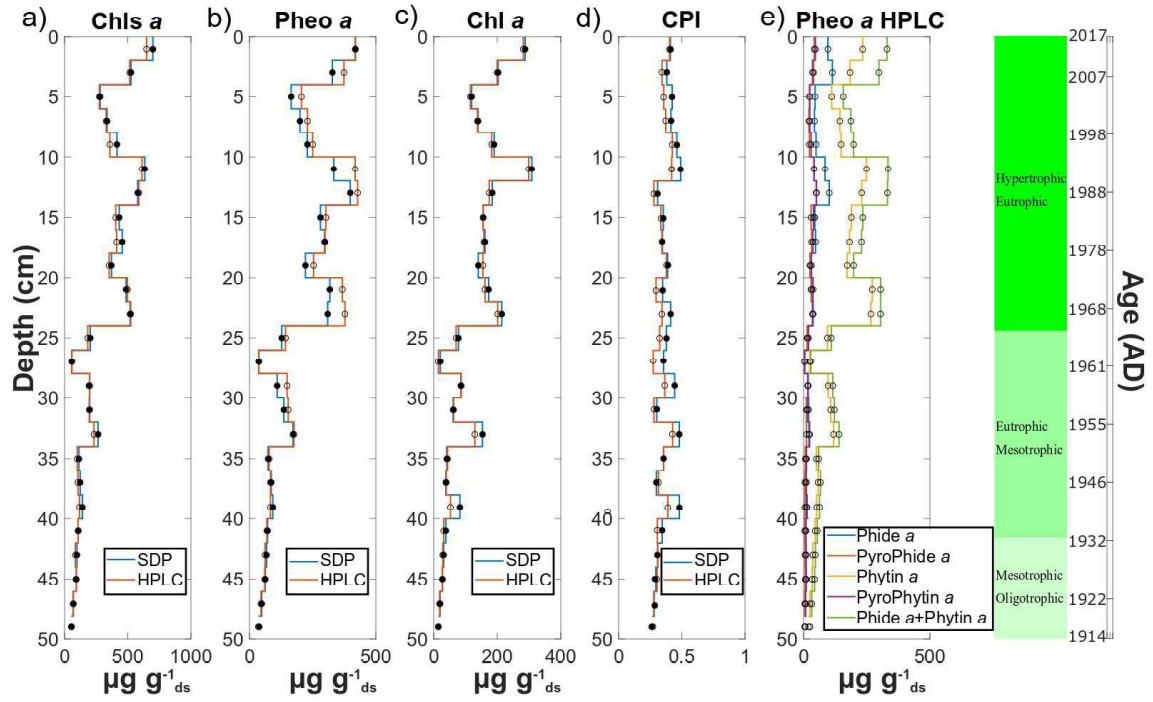
Fig.4



685

686

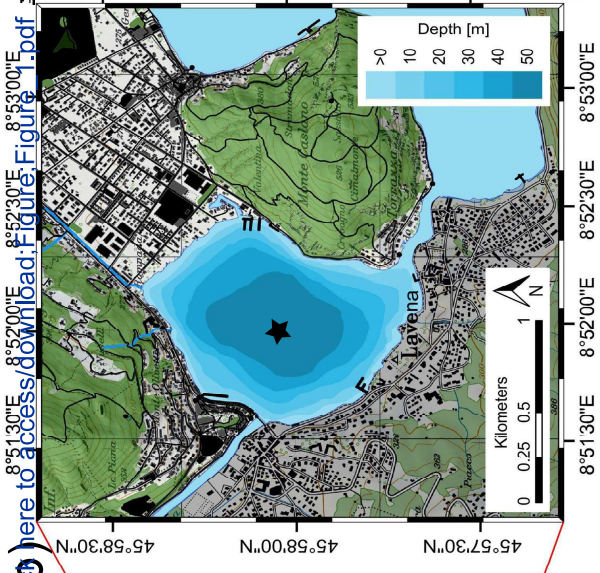
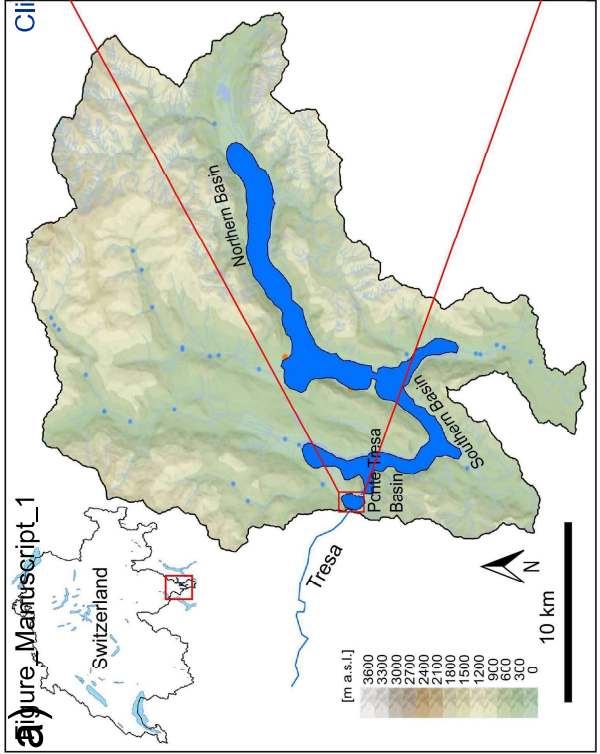
Fig. 5

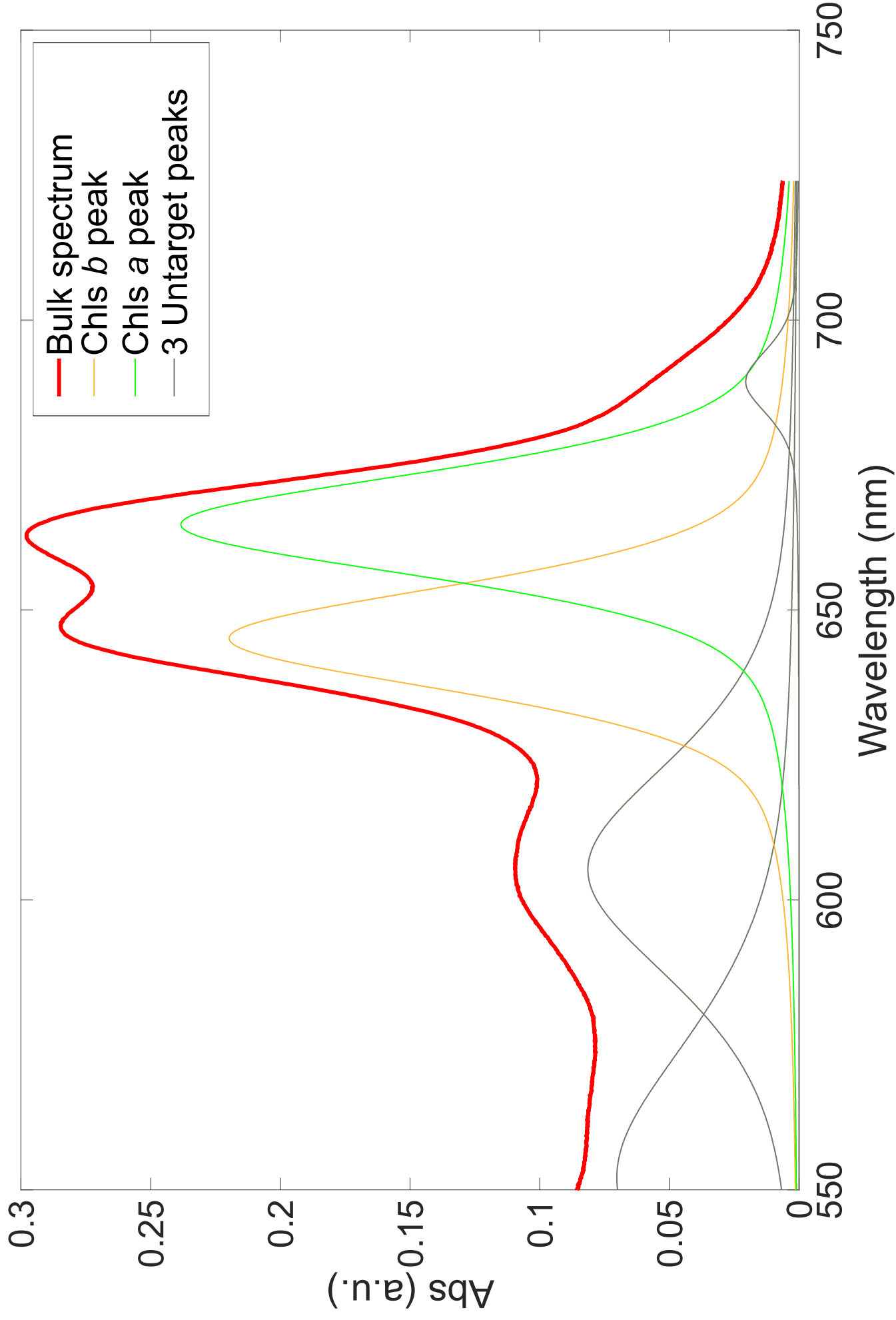


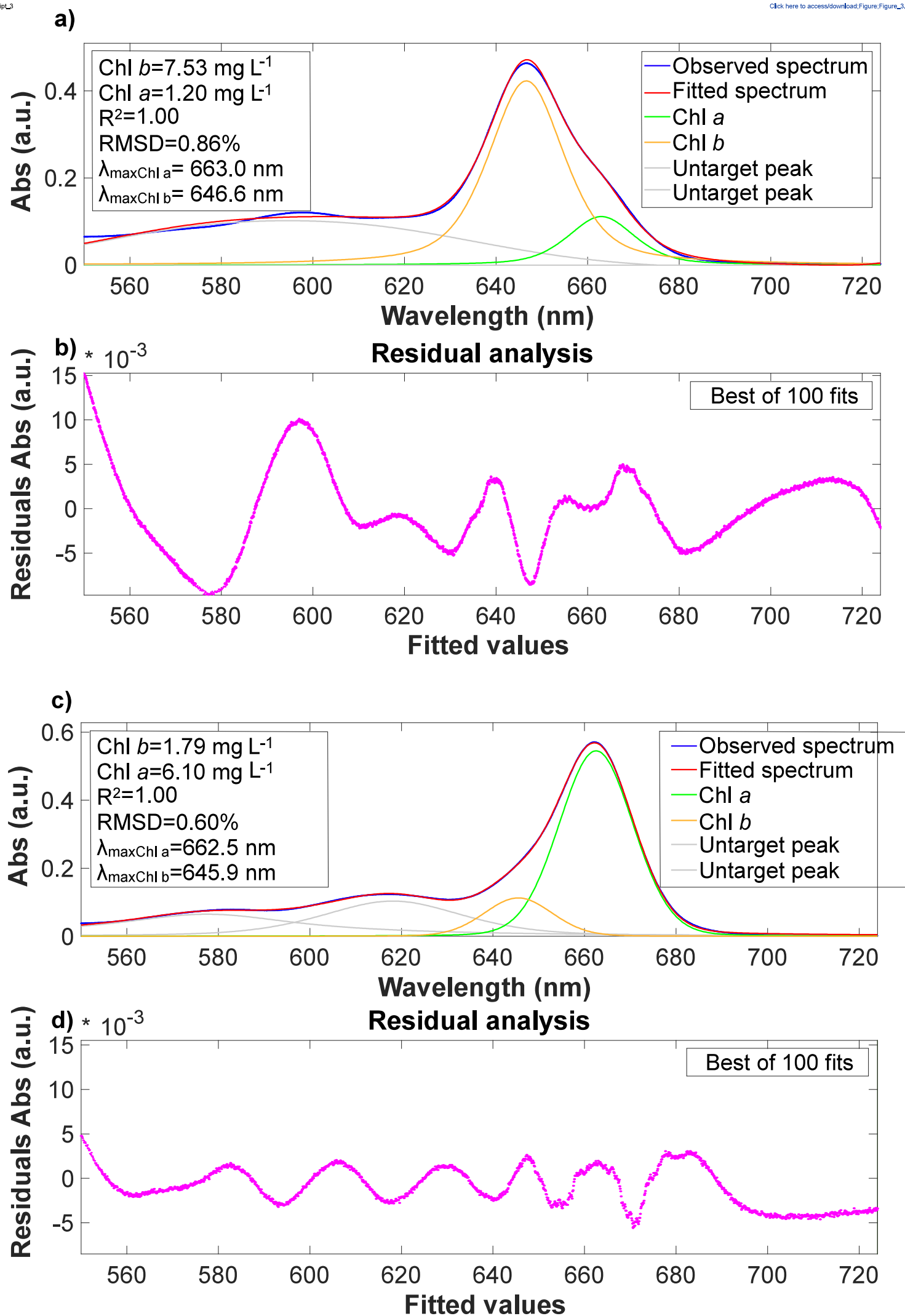
687

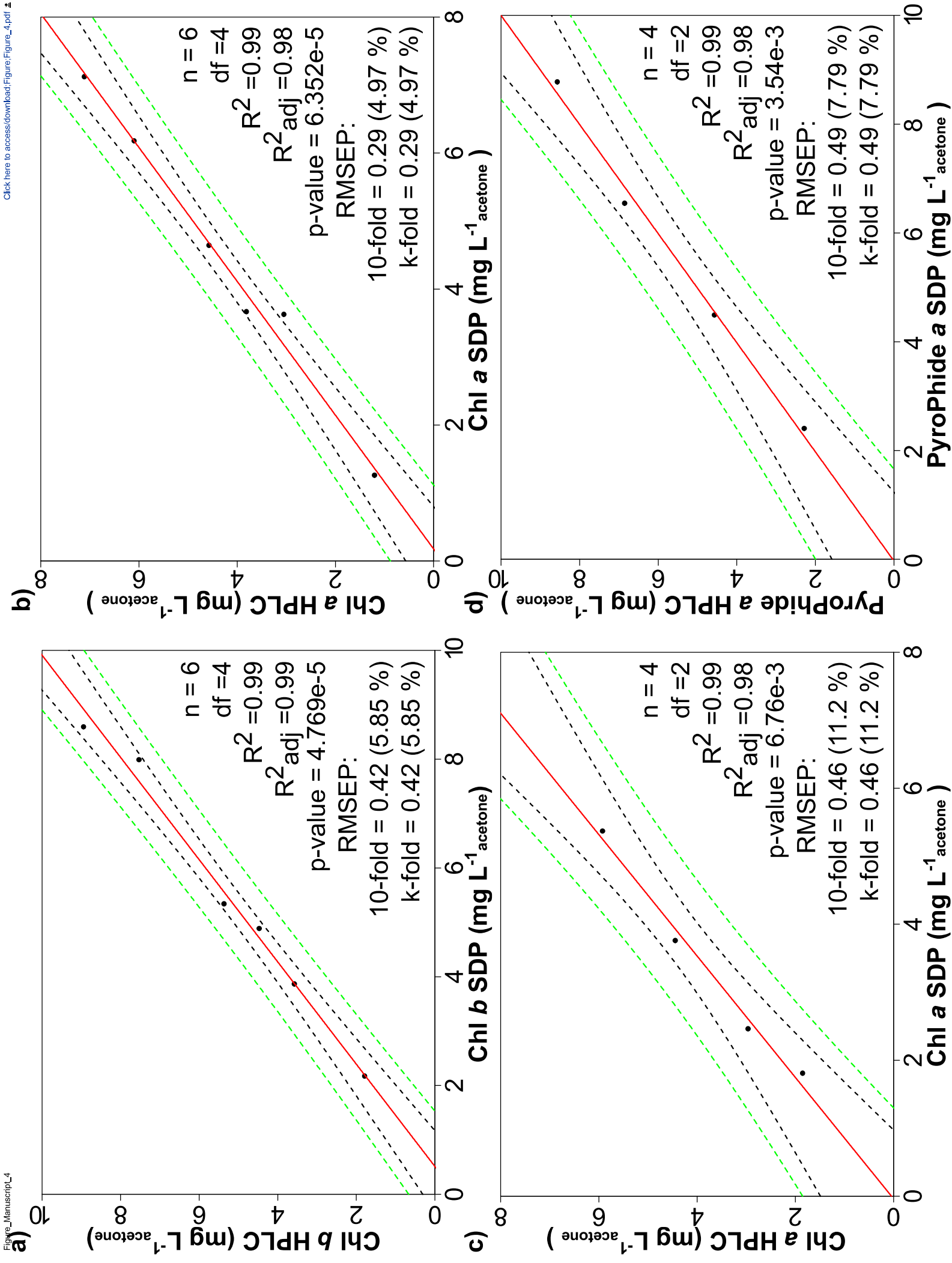
688 **Fig. 6**

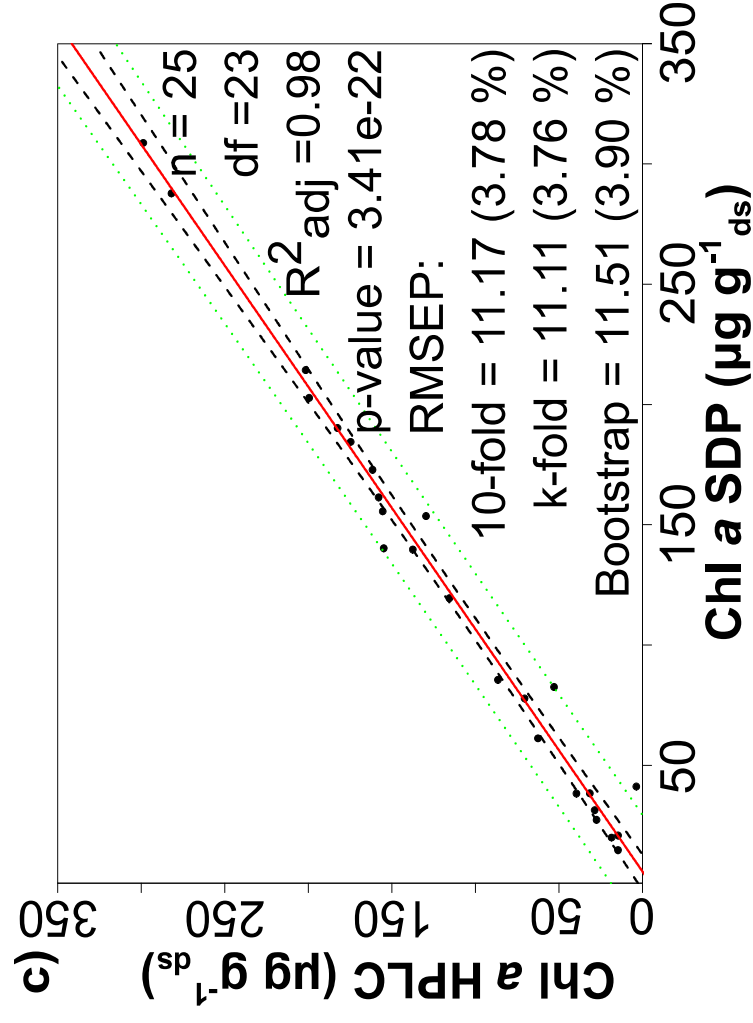
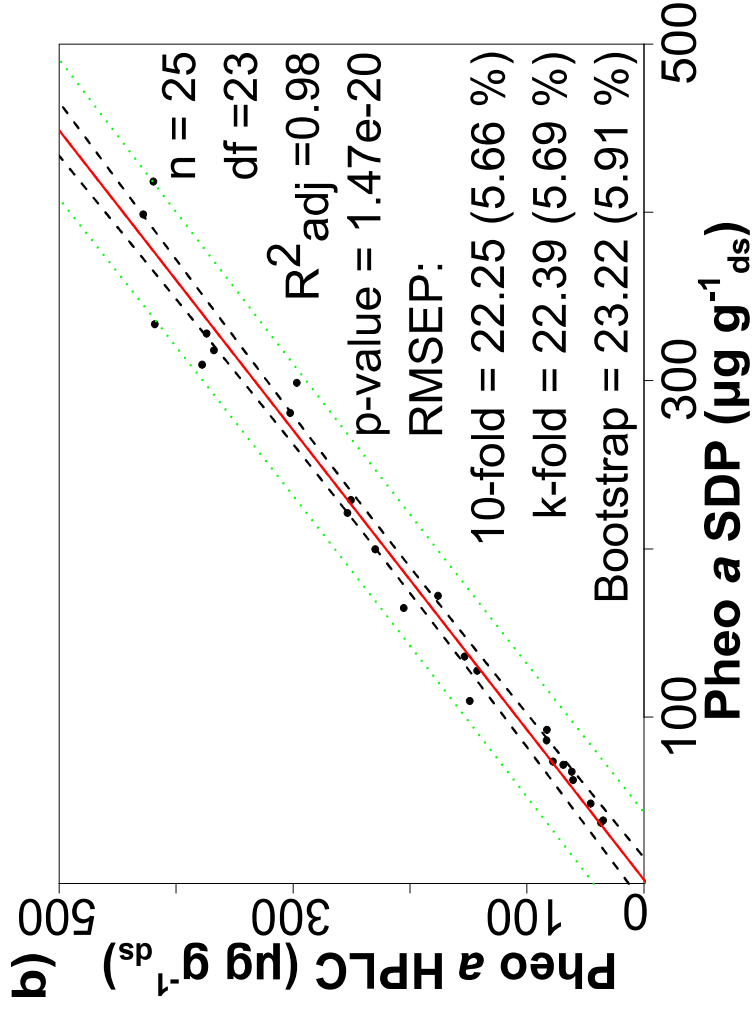
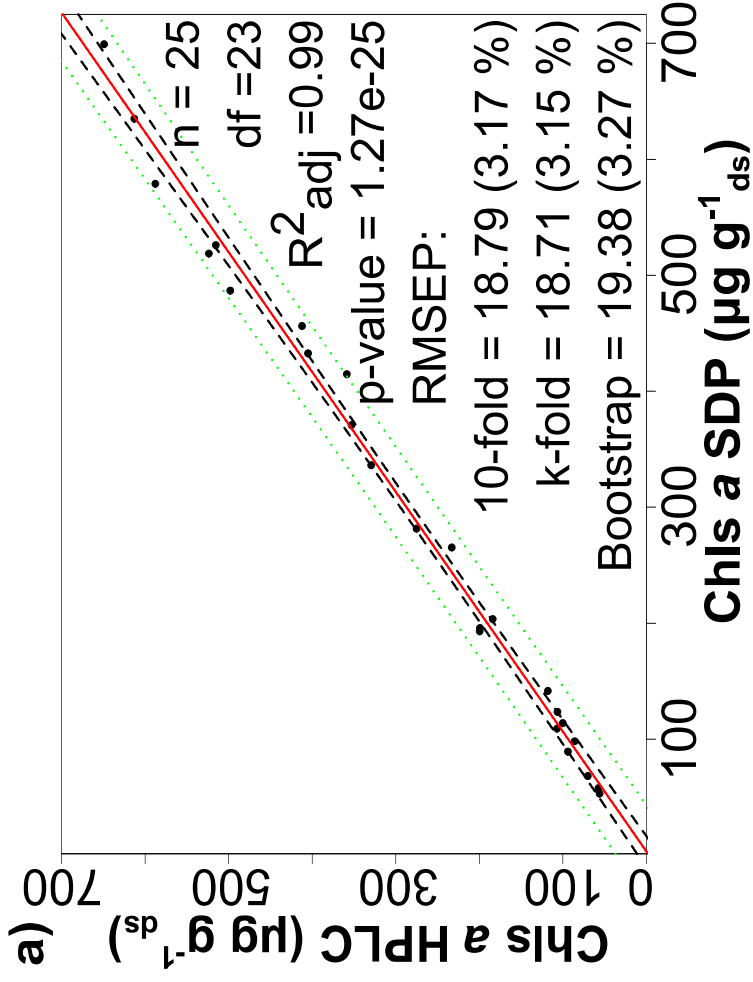
1
2
3
4
5
6
7
8
9
10
11
12
13
14
15
16
17
18
19
20
21
22
23
24
25
26
27
28
29
30
31
32
33
34
35
36
37
38
39
40
41
42
43
44
45
46
47
48
49
50
51
52
53
54
55
56
57
58
59
60
61
62
63
64
65

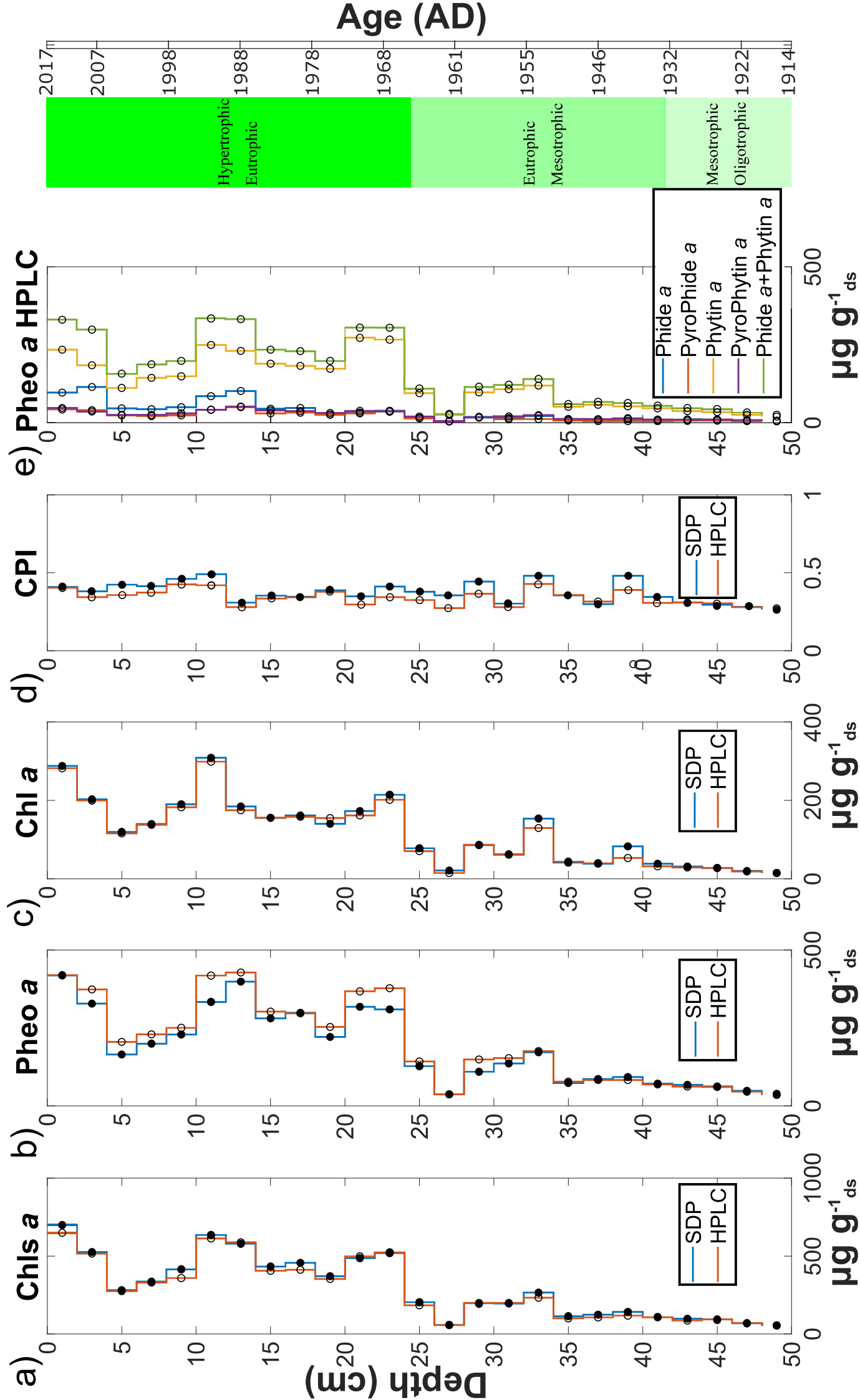












[Click here to view linked References](#)

Dear Andrea Sanchini,

Thank you for revision of your manuscript, "Quantification of chlorophyll a, chlorophyll b and pheopigments a in lake sediments through deconvolution of bulk UV-VIS absorption spectra" for the Journal of Paleolimnology.

You adopted the majority of recommended changes and offered good explanations for when you did not, which was an excellent response. On this last reading, however, I noticed very minor corrections that are needed for journal format requirements. The changes are too numerous to make successfully during proof corrections. I need to request one last minor revision that might take only 1 hour of your time, and it will prepare the manuscript to be accepted on the next submission.

There is a delay between the time when authors submit revisions, and the time when the revisions reach my assignments. For this reason, please wait 2-3 days after you submit your revision then write to me directly at whitmore@usf.edu to say that your last revision has been submitted. That message should hopefully reach me at the time the revision is posted, and I will be able to accept it.

Please attend to the following minor points, then resubmit:

Dear Dr. Thomas J. Whitmore

We would like to thank you again for your careful review. Below, you will find our detailed responses marked in blue colour text. We hope you will find our revisions adequate. Yes, once our revision is submitted, I will contact you again after 3 days to say that our revision has been submitted (email: whitmore@usf.edu).

Comment, Line 72: (Bianchi and Canuel 2011, McGowan 2013) needs a semicolon rather than a comma between the citations. Please check other citations in case such changes are needed, but I did not notice other such problems.

Response: *changed accordingly. We found other citations with mistakes, nevertheless now all the citations have been corrected. thank you.*

Comment, 2: There are small dots that appear between units in expressions that have several units, and the dots need to be replaced by spaces. For example, (L·cm⁻¹·mg⁻¹) needs to be changed to (L cm⁻¹ mg⁻¹), and there are many in the Standard Solutions Preparation section. The same for expressions such as L·cm⁻¹·mg⁻¹. Please scan the manuscript and make all such needed corrections throughout the manuscript. These are the corrections that are too numerous for us to make with proof corrections. Please also correct the units on Fig. 5 and Fig. 6 and replace those figures on the website, because we can not alter figures during proof corrections.

Response: *changed accordingly. We have removed all the small dots that appear between units throughout the text. We have also corrected Fig. 3, Fig. 4, Fig. 5, Fig. 6., ESM3, ESM4, ESM7 and ESM8.*

1
2
3
4
5
6
7
8
9
10
11
12
13
14
15
16
17
18
19
20
21
22
23
24
25
26
27
28
29
30
31
32
33
34
35
36
37
38
39
40
41
42
43
44
45
46
47
48
49
50
51
52
53
54
55
56
57
58
59
60
61
62
63
64
65

Comment, 3: It is ok to leave out the expression "Electronic Supplementary Material" if you wish and to just show the ESM number, e.g., ESM1, but you might want to include that the first time you refer to ESM material if you think that will be clearer

Response: *we have decided to include the expression "Electronic Supplementary Material" only the first time we refer to ESM material. Thank you.*

Comment, 4: Line 416: a space is needed between the figure subpanels in Fig. 6a,c, so Fig. 6a, c

Response: *changed accordingly.*

Please submit your revised manuscript online using the Editorial Manager system (and contact me as described above).

Your username is: asanchini

If you forgot your password, you can click the 'Send Login Details' link on the EM Login page at <https://www.editorialmanager.com/jopl/>

Thank you.

With kind regards,

Thomas J. Whitmore

JOPL Co-Editor in Chief

whitmore@usf.edu

[Click here to view linked References](#)

1 **Electronic Supplementary Material to:**

2 **Quantification of chlorophyll *a*, chlorophyll *b* and pheopigments *a* in lake sediments**
3 **through deconvolution of bulk UV-VIS absorption spectra**

4
5
6
7 5 Andrea Sanchini^{1,2*}, Martin Grosjean^{1,2}

8
9 6 1 Oeschger Centre for Climate Change Research, University of Bern, 3012 Bern, Switzerland

10
11 7 2 Institute of Geography, University of Bern, Hallerstrasse 12, 3012 Bern, Switzerland

12
13
14 9 *** Corresponding author:**

15
16 10

17
18 11 Andrea Sanchini

19
20 12 University of Bern

21
22 13 Hallerstrasse 12

23
24 14 3012 Bern, Switzerland

25
26 15 andrea.sanchini@giub.unibe.ch

27 16

28
29 17 **Co-Author:**

30
31 18

32
33 19 Martin Grosjean

34
35 20 martin.grosjean@oeschger.unibe.ch

36 21

37
38 22

39
40 23

41
42 24

43
44 25

45
46 26

47
48 27

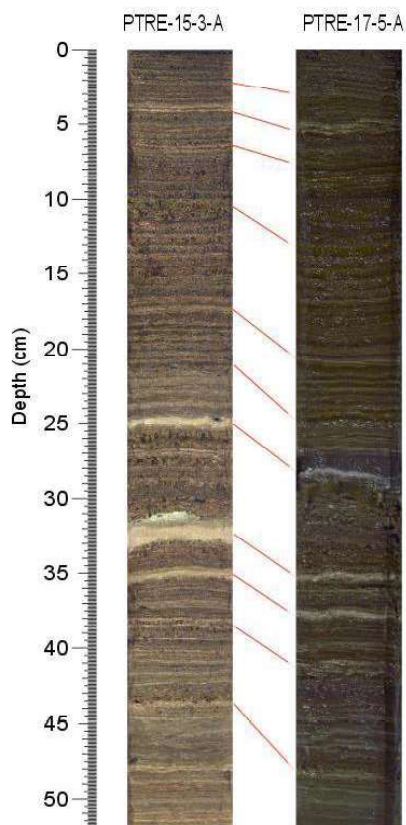
49
50 28

51
52 29

53
54 30

55
56 31

57
58
59
60
61
62
63
64
65



Depth (cm)	Mean age (CE)	Uncertainty (-)	Uncertainty (+)
0-2	2014	2010	2017
2-4	2007	2004	2010
4-6	2003	2002	2004
6-8	2000	1998	2002
8-10	1995	1993	1998
10-12	1991	1990	1993
12-14	1988	1987	1990
14-16	1985	1983	1987
16-18	1981	1978	1983
18-20	1975	1973	1978
20-22	1971	1969	1973
22-24	1967	1964	1969
24-26	1963	1962	1964
26-28	1961	1960	1962
28-30	1959	1958	1960
30-32	1957	1955	1958
32-34	1953	1952	1955
34-36	1950	1948	1952
36-38	1946	1944	1948
38-40	1942	1939	1944
40-42	1935	1932	1939
42-44	1930	1927	1932
44-46	1925	1922	1927
46-48	1921	1919	1922
48-50	1917	1914	1919

32
33 **ESM1** Stratigraphic correlation between PTRE-17-5-A (this study) and the dated short core
34 PTRE-15-3-A described in Schneider et al. (2018).
35

36 **ESM2** Extraction method

37 First, the samples were freeze-dried, then ground and homogenized with a stainless steel
38 spatula. Circa 0.5 g of dry sediment was extracted with 5 mL of acetone HPLC grade 95%
39 following a triple sequential extraction cycle, each composed of vortex (1 minute), sonication
40 (1 minute) and centrifugation (10 min, 5000 rpm). After the solid-liquid extraction, the water
41 in the supernatant was removed by passing it through a glass column filled with (from the
42 bottom to the top): glass wool (pretreated in a muffle furnace), 3 g of Dionex™ ASE™ Prep
43 DE, 1 g of Dionex™ ASE™ Prep MAP, 1 g of Dionex™ ASE™ Prep DE and glass wool
44 again on the top. We pre- and post-conditioned each column with 10 mL of acetone HPLC
45 grade 95%. The water-free supernatant was dried under a N₂ stream on a heating plate set at 35
46 °C to speed up the solvent pre-concentration. Afterwards, the extract was reconstituted with
47 acetone HPLC grade 100%, filtered (0.2 μm, Nylon, Fisher Brand) and stored in a freezer at -
48 20 °C until further analysis. Recovery and repeatability of the extraction method was assessed
49 in eight burned (550°C) sediment samples spiked with chl *a*. The recovery rate is 74% with a
50 relative standard deviation (RSD) of 4%.

51

52 **ESM3** HPLC Operating Conditions: Mobile phase A= 80:20 v/v % (MeOH: aqueous solution)
 53 of 0.001 M ion pairing (Tetrabutylammonium phosphate monobasic solution 1.0 M in H₂O)
 54 and 0.001 M of propionic acid. Mobile phase B= 60:40 v/v % (Acetone: Methanol). The flow
 55 rate increases linearly (1mL min⁻¹ to 2mL min⁻¹) between 0 to 65 minutes and decreases linearly
 56 (2mL min⁻¹ to 1mL min⁻¹) between 69 to 79 minutes.

HPLC Operating Conditions

Retention time (min)	Flow rate (mL min ⁻¹)	Solvent composition (v/v %)	
		A	B
0	1	80	20
20		65	35
25		65	35
65	2	0	100
69	2	0	100
75	1	80	20
79	1	80	20

57

58 **ESM4** Analytical standards used in the spectrophotometric and HPLC analyses.

List of Analytical standards

Compounds	Company, manufacturing location	Purity, State
Chlorophyll <i>a</i>	Sigma-Aldrich, Buchs, Switzerland	99.5% HPLC, powder
Chlorophyll <i>b</i>	Sigma-Aldrich, Buchs, Switzerland	99.3% HPLC, powder
Pyropheophorbide <i>a</i>	Santa Cruz, Biotechnology	95% UV, powder
Chlorophyll <i>c2</i>	DHI, Copenhagen, Denmark	0.936 mg L ⁻¹ , liquid
Pheophytin <i>a</i>	DHI, Copenhagen, Denmark	3.356 mg L ⁻¹ , liquid
Pheophorbide <i>a</i>	DHI, Copenhagen, Denmark	3.125 mg L ⁻¹ , liquid

59

60

61

62

63

1
2
3
4
5
6
7
8
9
10
11
12
13
14
15
16
17
18
19
20
21
22
23
24
25
26
27
28
29
30
31
32
33
34
35
36
37
38
39
40
41
42
43
44
45
46
47
48
49
50
60
61
62
63
64
65

64 **ESM5** Functions tested for the best fit between the individual absorbance spectra and the
 65 predicted one for each of the target pigments.

Functions tested in the INLLS method (O'Haver 2016)

Symmetrical functions	Single Gaussian
	Two Gaussians
	Single Lorentzian
	Logistic distribution
	Voigt profile
	Single Pearson
	Gauss/Lorentz blend
Asymmetrical functions	One Gaussian
	Two Gaussians
	Exp. modified Gaussian
	BiGaussian
	Exponential pulse
	Alpha function

66 The Gaussian/Lorentzian blend function (GL) is composed of a Gaussian (1) and a Lorentzian
 67 (2) function in different percentuals (m):

$$68 \quad GL(\lambda, \delta, \omega, m) = \frac{m}{100} * G(\lambda, \delta, \omega) + \left(1 - \frac{m}{100}\right) * L(\lambda, \delta, \omega)$$

$$69 \quad G(\lambda, \delta, \omega) = e \left(-\frac{(\lambda-\delta)^2}{2\omega^2} \right) \quad (1)$$

$$70 \quad L(\lambda, \delta, \omega) = \frac{\omega^2}{\omega^2 + (\lambda-\delta)^2} \quad (2)$$

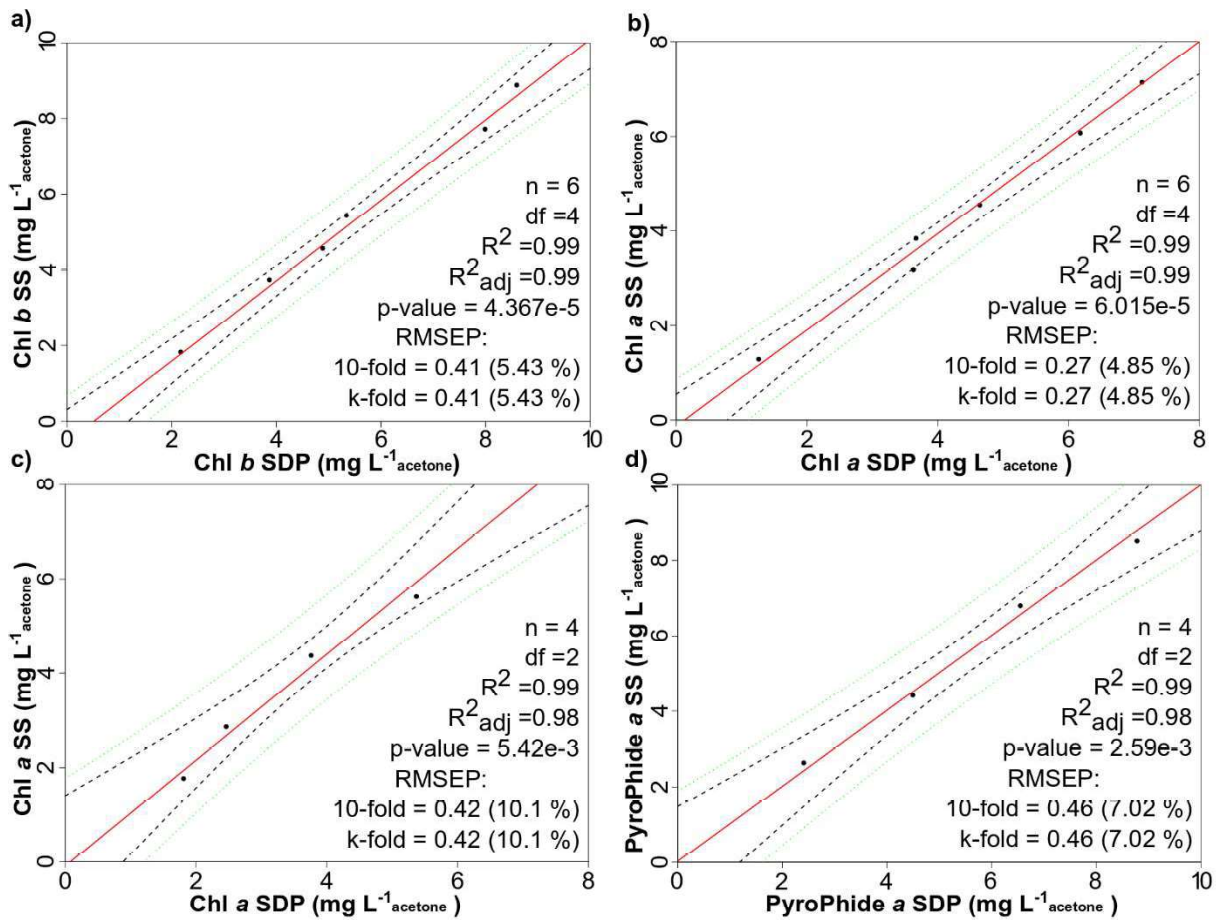
73 **ESM6** Comparison between the INLLS fitted and observed spectra of singles pure standards.
 74 UV-VIS Absorption Spectra of target pigments were measured in acetone 100%.

INLLS Comparison					
Guass/Lorentz blend function	chl <i>a</i>	chl <i>b</i>	pyrophide <i>a</i>	phytin <i>a</i>	phide <i>a</i>
R²	0.99	0.98	0.99	0.99	0.99
RMSD %	2.64	4.50	2.81	3.21	3.29

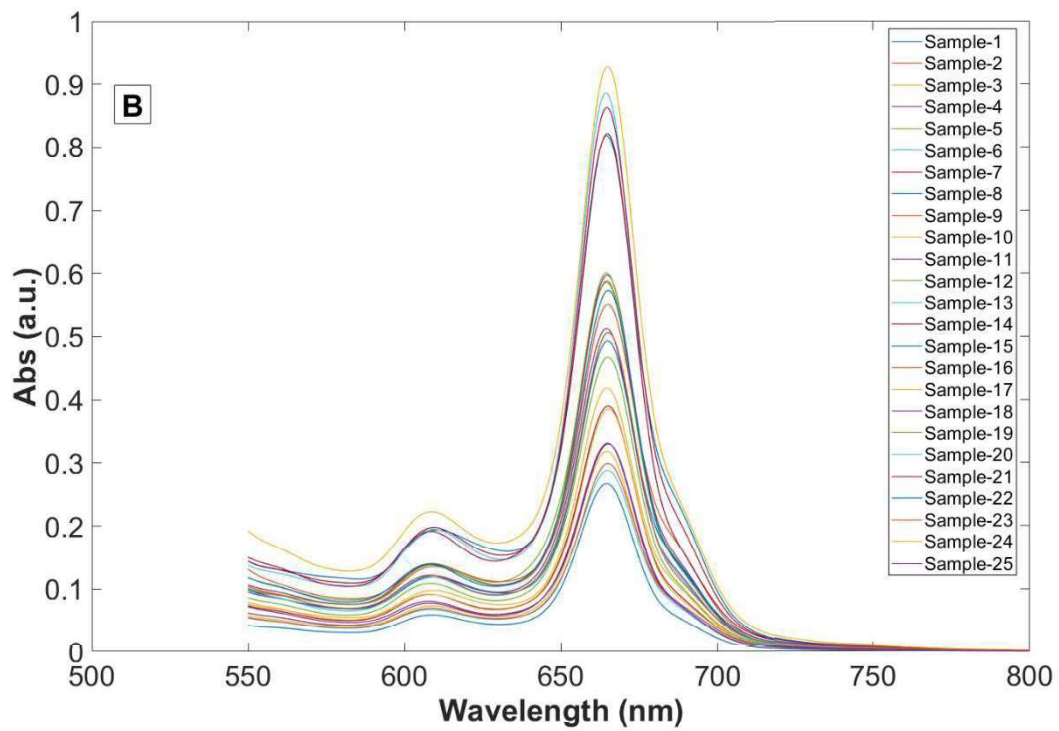
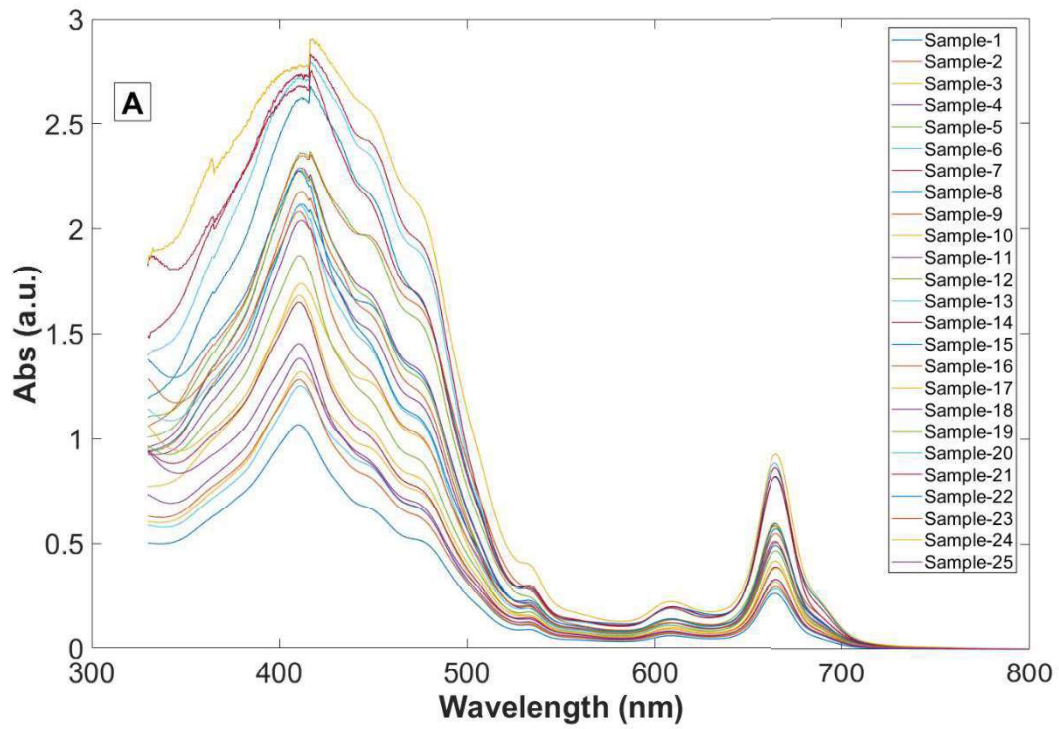
80 **ESM7** Maximum wavelength of absorption of the target pigments measured in the UV-VIS
 81 absorption spectral range in acetone 100% solutions.

Maxima in the UV-VIS absorption spectra of target pigments					
Solvent:	chl <i>a</i>	chl <i>b</i>	pyrophide <i>a</i>	phytin <i>a</i>	phide <i>a</i>
Acetone 100%					
λ_{\max} (nm)	431.1, 662.4	458.0, 645.7	410, 666.5	409.7, 665.7	410.2, 666.2
(λ_{\max}) ($1 \text{ M}^{-1} \text{ cm}^{-1}$)	96048, 78750	130499, 47028	75876, 44721	100350, 44600	97733, 44251

82
 83 **ESM8** Method validation between Standard Solution SS values and SDP calculated
 84 concentrations for (a-b) seven standard solutions with mixtures of chl *a* and chl *b* and (c-d) four
 85 standard solutions with mixtures of chl *a* and pyropheorbide *a*. The black dashed lines delimit
 86 the 95% confidence interval for the regression function (red) and the green lines indicate the
 87 range of the predicted values (green).

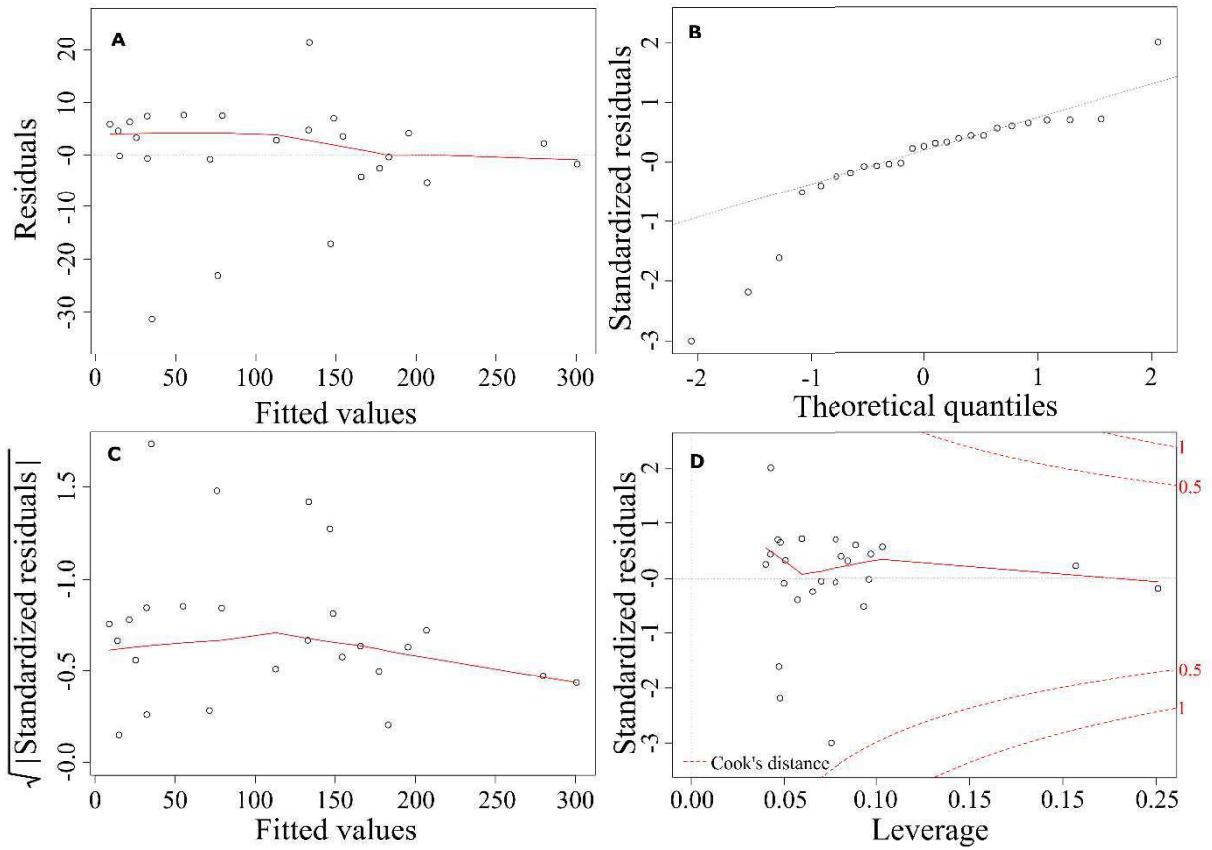


88



89
 90 **ESM9** UV-VIS absorbance spectra of 25 samples from the PTRE 17-5 sediment core: A)
 91 Absorption range from 350 nm to 800 nm; B) Absorption range from 550 nm to 800 nm.

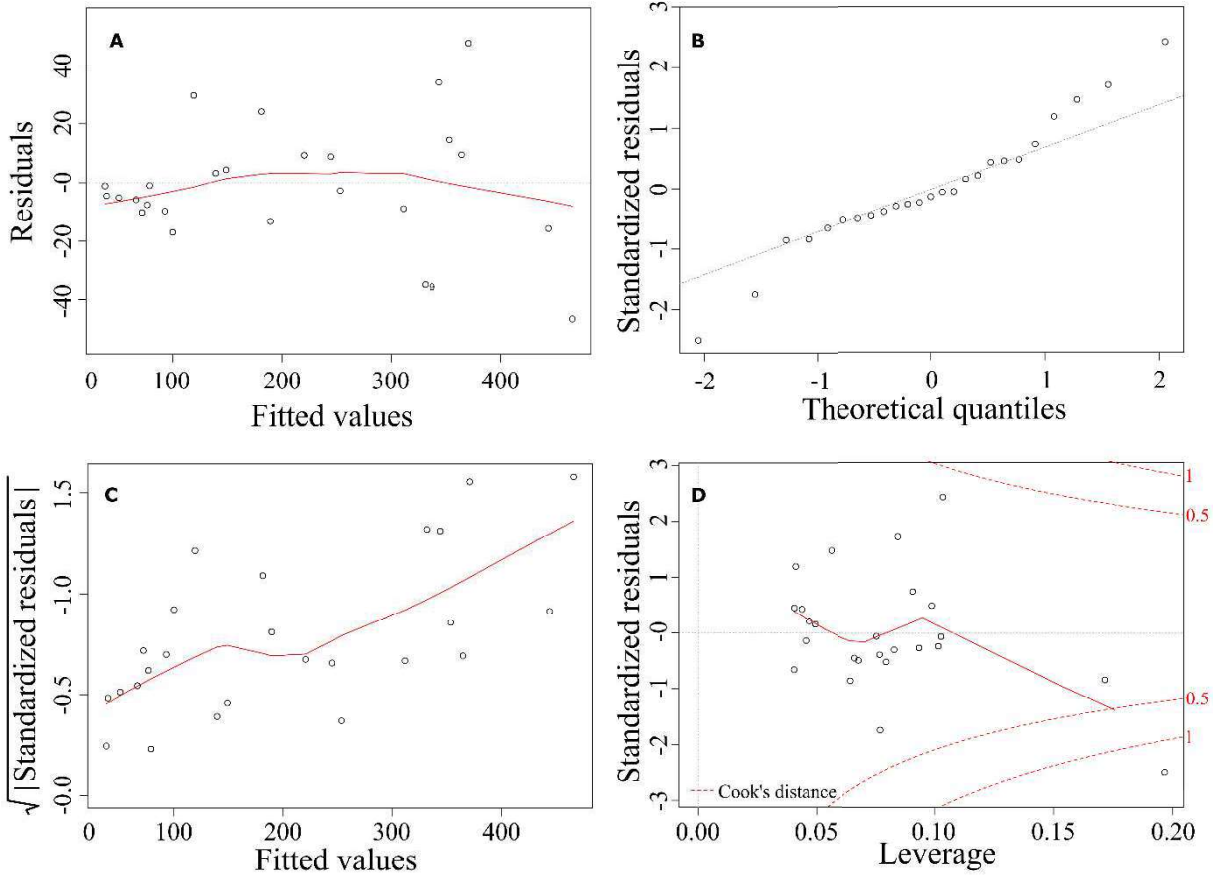
92
 93
 94
 95
 96
 97
 98
 99
 100



93
 94
 95
 96
 97

ESM10 Residual analysis of chl *a* from the PTRE 17-5 sediment samples (n=25) showing A) residuals versus fitted values (Abs, a.u.), B) standardized residuals versus theoretical quantiles (normal Q–Q plot), C) scale-location plot, and D) standardized residuals versus leverage plot

1
 2
 3
 4
 5
 6
 7
 8
 9
 10
 11
 12
 13
 14
 15
 16
 17
 18
 19
 20
 21
 22
 23
 24
 25
 26
 27
 28
 29
 30
 31
 32
 33
 34
 35
 36
 37
 38
 39
 40
 41
 42
 43
 44
 45
 46
 47
 48
 49
 50
 51
 52
 53
 54
 55
 56
 57
 58
 59
 60
 61
 62
 63
 64
 65

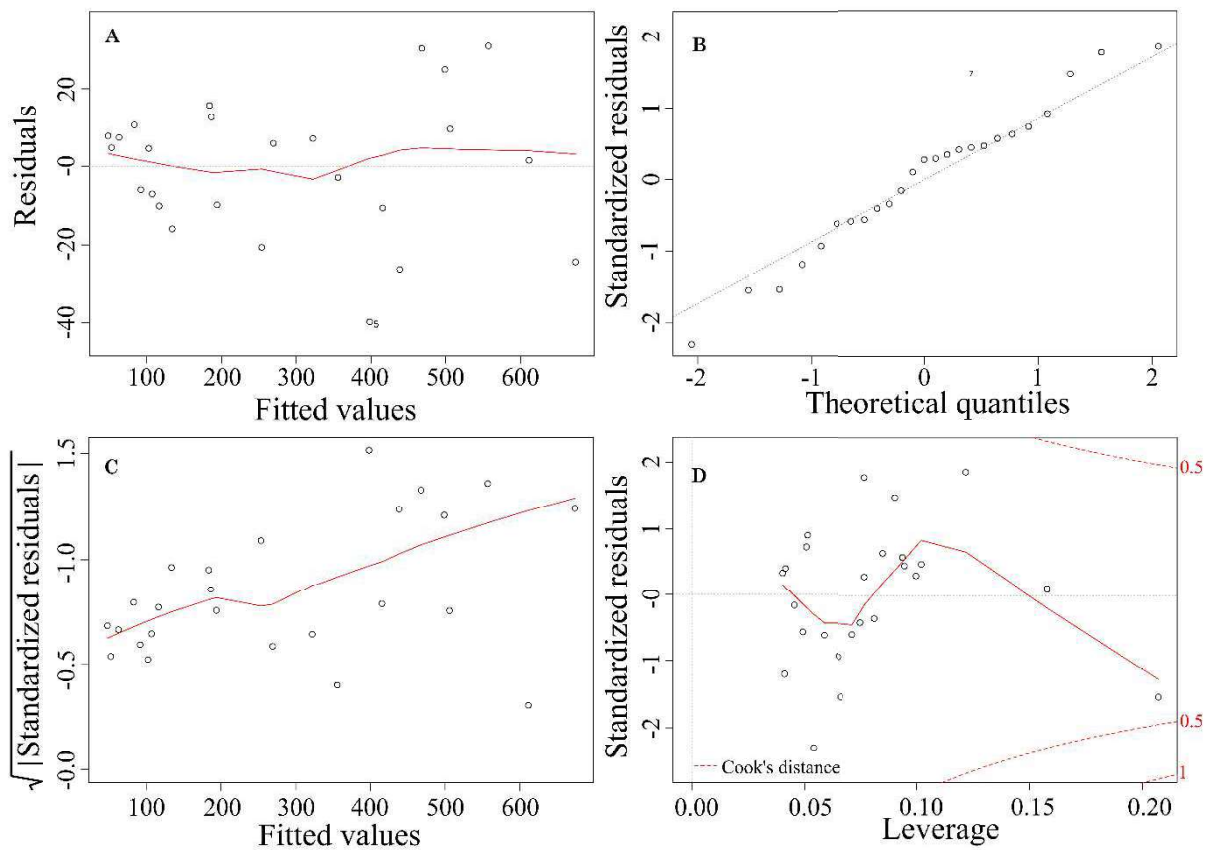


98

99 **ESM11** Residual analysis of pheo *a* from the PTRE 17-5 sediment samples (n=25) showing A)
 100 residuals versus fitted values (Abs, a.u.), B) standardized residuals versus theoretical quantiles
 101 (normal Q–Q plot), C) scale-location plot, and D) standardized residuals versus leverage plot.

102

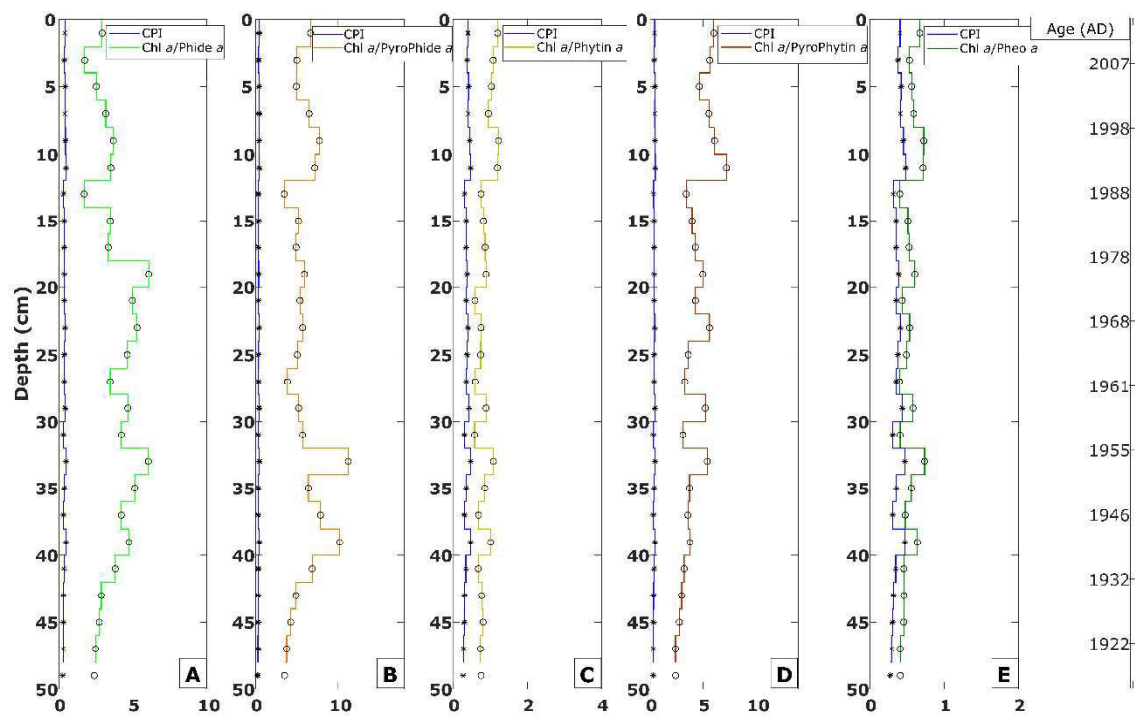
1
2
3
4
5
6
7
8
9
10
11
12
13
14
15
16
17
18
19
20
21
22
23
24
25
26
27
28
29
30
31
32
33
34
35
36
37
38
39
40
41
42
43
44
45
46
47
48
49
50
51
52
53
54
55
56
57
58
59
60
61
62
63
64
65



103

104 **ESM12** Residual analysis of chl *a* from the PTRE 17-5 sediment samples showing A) residuals
 105 versus fitted values (Abs, a.u.), B) standardized residuals versus theoretical quantiles (normal
 106 Q-Q plot), C) scale-location plot, and D) standardized residuals versus leverage plot.

1
2
3
4
5
6
7
8
9
10
11
12
13
14
15
16
17
18
19
20
21
22
23
24
25
26
27
28
29
30
31
32
33
34
35
36
37
38
39
40
41
42
43
44
45
46
47
48
49
50
51
52
53
54
55
56
57
58
59
60
61
62
63
64
65



ESM13 PTRE 17-5-A stratigraphy comparing CPI values (blue lines) against individual and total chl *a*/pheo *a* ratios from HPLC measurements. A) calculated CPI values against chl *a*/phide *a* HPLC concentration ratios, B) calculated CPI values against chl *a*/pyrophide *a* HPLC concentration ratios, C) calculated CPI values against chl *a*/phytin *a* HPLC concentration ratios, D) calculated CPI values against chl *a*/pyrophytin *a* HPLC concentration ratios and E) calculated CPI against chl *a*/pheo *a* HPLC values.

References

O'Haver T (2016). A Pragmatic Introduction to Signal Processing. Lulu Enterprises Incorporated.

44 attachment to manuscript_SI_ESM3 [Click here to access/download;attachment to manuscript;ESM3.pdf](#) 

45 [Click here to view linked References](#)

46

47

HPLC Operating Conditions

Retention time (min)	Flow rate (mL min ⁻¹)	Solvent composition (v/v %)
0	1	A 80 B 20
20		65 35
25		65 35
65	2	0 100
69	2	0 100
75	1	80 20
79	1	80 20

63

64

65

36 attachment to manuscript_SI_ESM4

Click here to access/download:attachment to manuscript;ESM4.pdf



38 Click [here to view linked References](#)

	List of Analytical standards		
	Compounds	Company, manufacturing location	Purity, State
40			
41			
42			
43			
44			
45			
46	Chlorophyll <i>a</i>	Sigma-Aldrich, Buchs, Switzerland	99.5% HPLC, powder
47			
48	Chlorophyll <i>b</i>	Sigma-Aldrich, Buchs, Switzerland	99.3% HPLC, powder
49			
50			
51			
52	Bacteriochlorophyll <i>a</i>	Sigma-Aldrich, St. Louis, USA	Circa 60% UV, powder
53			
54	Pyropheophorbide <i>a</i>	Santa Cruz, Biotechnology	95% UV, powder
55			
56			
57	Chlorophyll <i>c2</i>	DHI, Copenhagen, Denmark	0.936 mg L ⁻¹ , liquid
58			
59	Pheophytin <i>a</i>	DHI, Copenhagen, Denmark	3.356 mg L ⁻¹ , liquid
60			
61			
62	Pheophorbide <i>a</i>	DHI, Copenhagen, Denmark	3.125 mg L ⁻¹ , liquid
63			
64			
65			

32 [Click here to view linked References](#)

33 **Functions tested in the INLLS method (O'Haver 2016)**

34 **Symmetrical**

35 **functions**

36 Single Gaussian

37 Two Gaussians

38 Single Lorentzian

39 Logistic distribution

40 Voigt profile

41 Single Pearson

42 Gauss/Lorentz blend

43 One Gaussian

44 Two Gaussians

45 Exp. modified Gaussian

46 BiGaussian

47 Exponential pulse

48 Alpha function

49

50

51

52

53

The Gaussian/Lorentzian blend function (GL) is composed of a Gaussian (1) and a Lorentzian

54

55 (2) function in different percentuals (m):

56

$$GL(\lambda, \delta, \omega, m) = \frac{m}{100} * G(\lambda, \delta, \omega) + \left(1 - \frac{m}{100}\right) * L(\lambda, \delta, \omega)$$

57

58

59

60

61

62

63

64

65

$$G(\lambda, \delta, \omega) = e^{-\left(-\frac{(\lambda-\delta)^2}{2\omega^2}\right)}$$

$$L(\lambda, \delta, \omega) = \frac{\omega^2}{\omega^2 + (\lambda - \delta)^2}$$

(1)

(2)

53 attachment to manuscript_SI_ESM6 [Click here to access/download;attachment to manuscript;ESM6.pdf](#) 54

55 [Click here to view linked References](#) 56

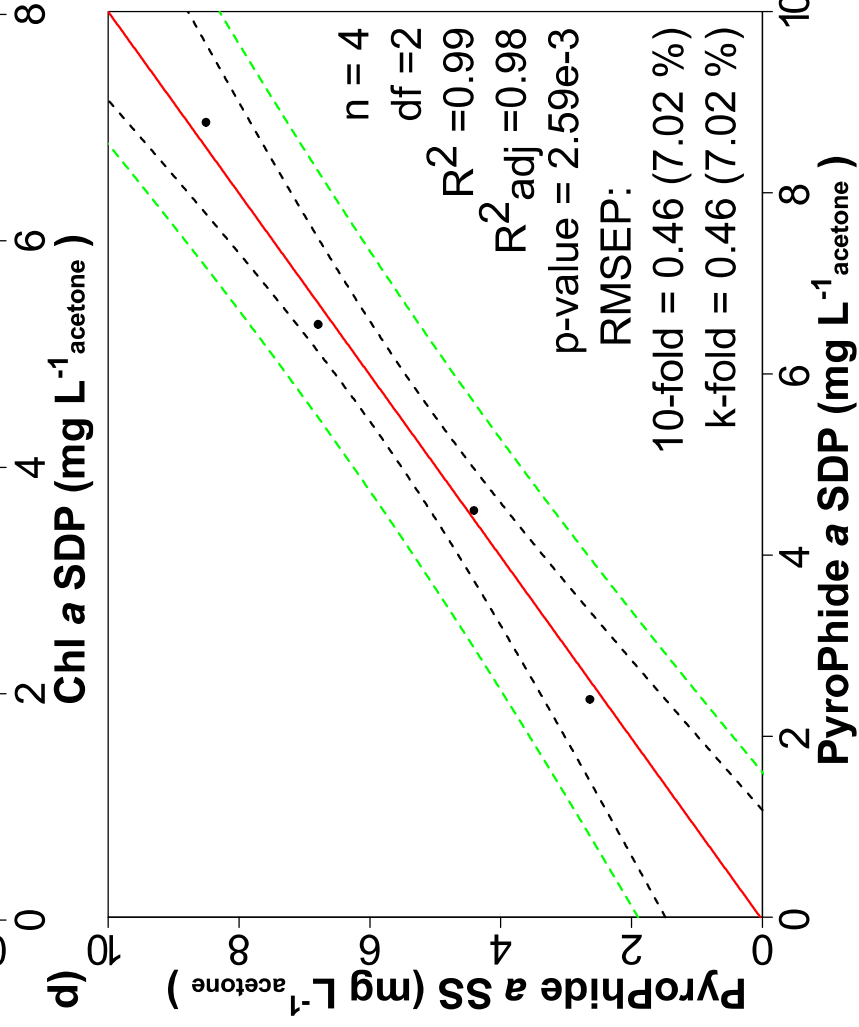
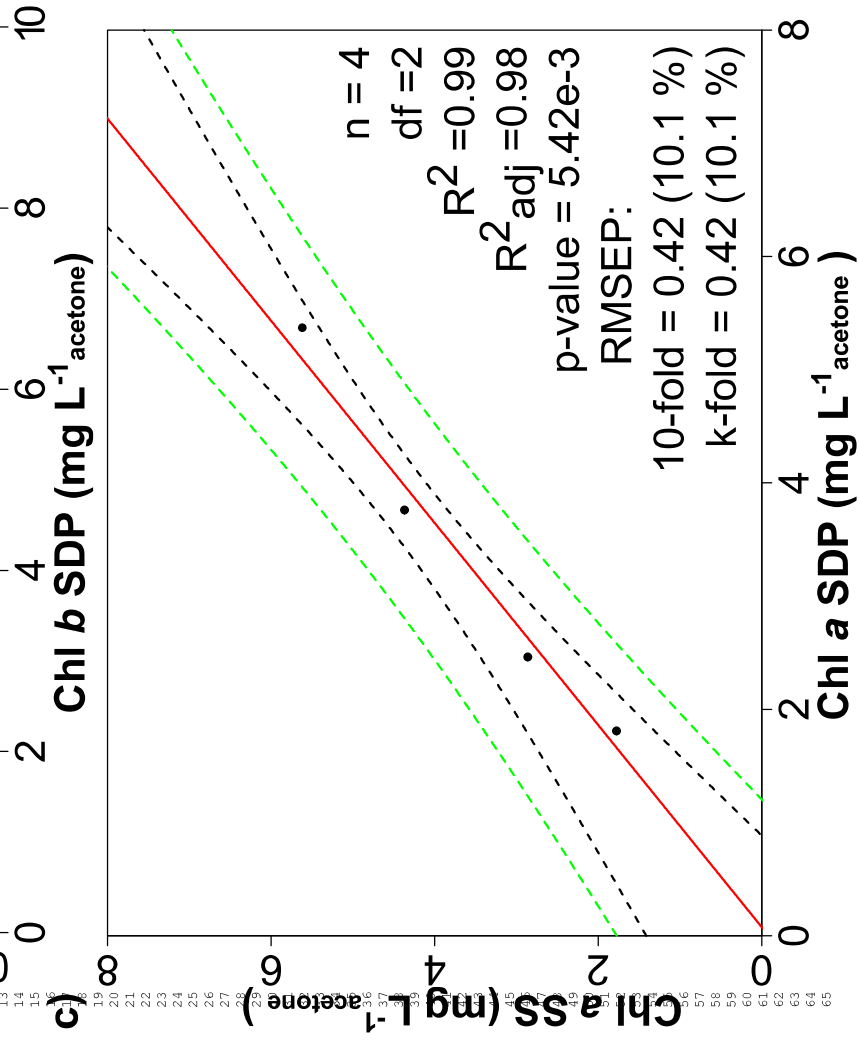
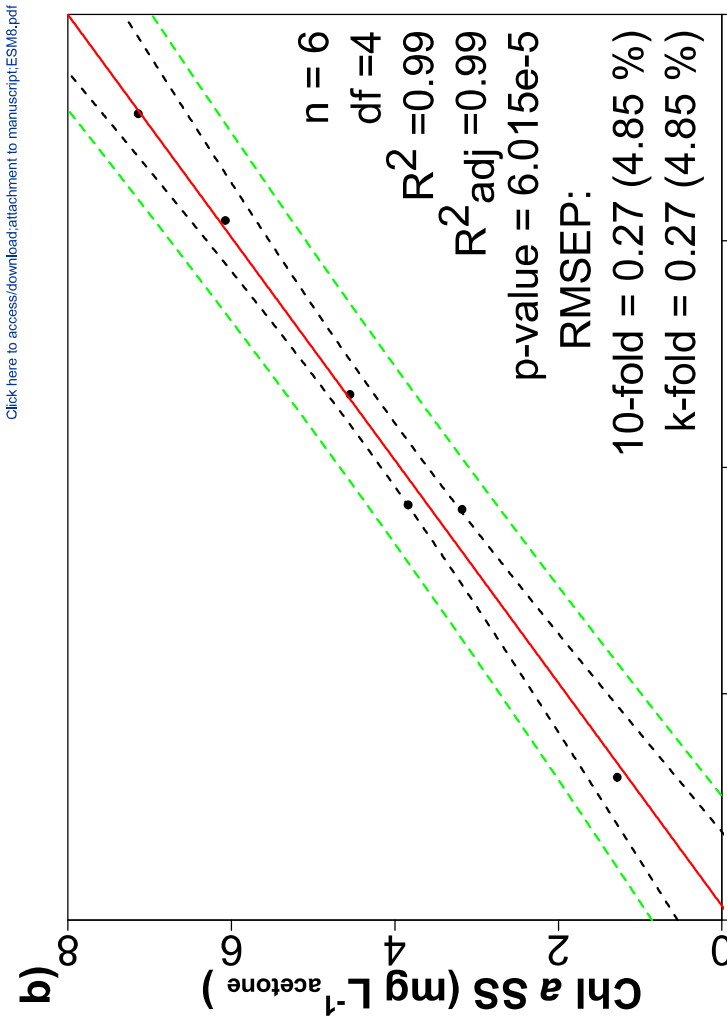
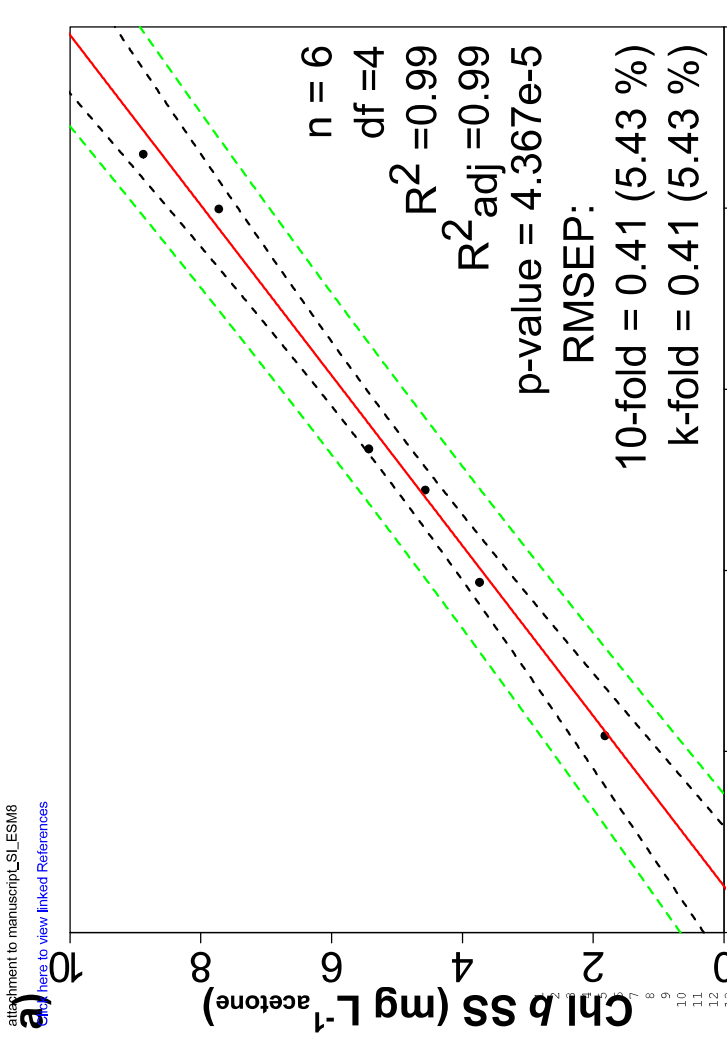
INLLS Comparison							
Guass/Lorentz blend function	R²	RMSD %	<i>chl a</i>	<i>chl b</i>	<i>pyrophide a</i>	<i>phytin a</i>	<i>phide a</i>
	0.99	2.64		0.98	0.99	0.99	0.99
				4.50	2.81	3.21	3.29

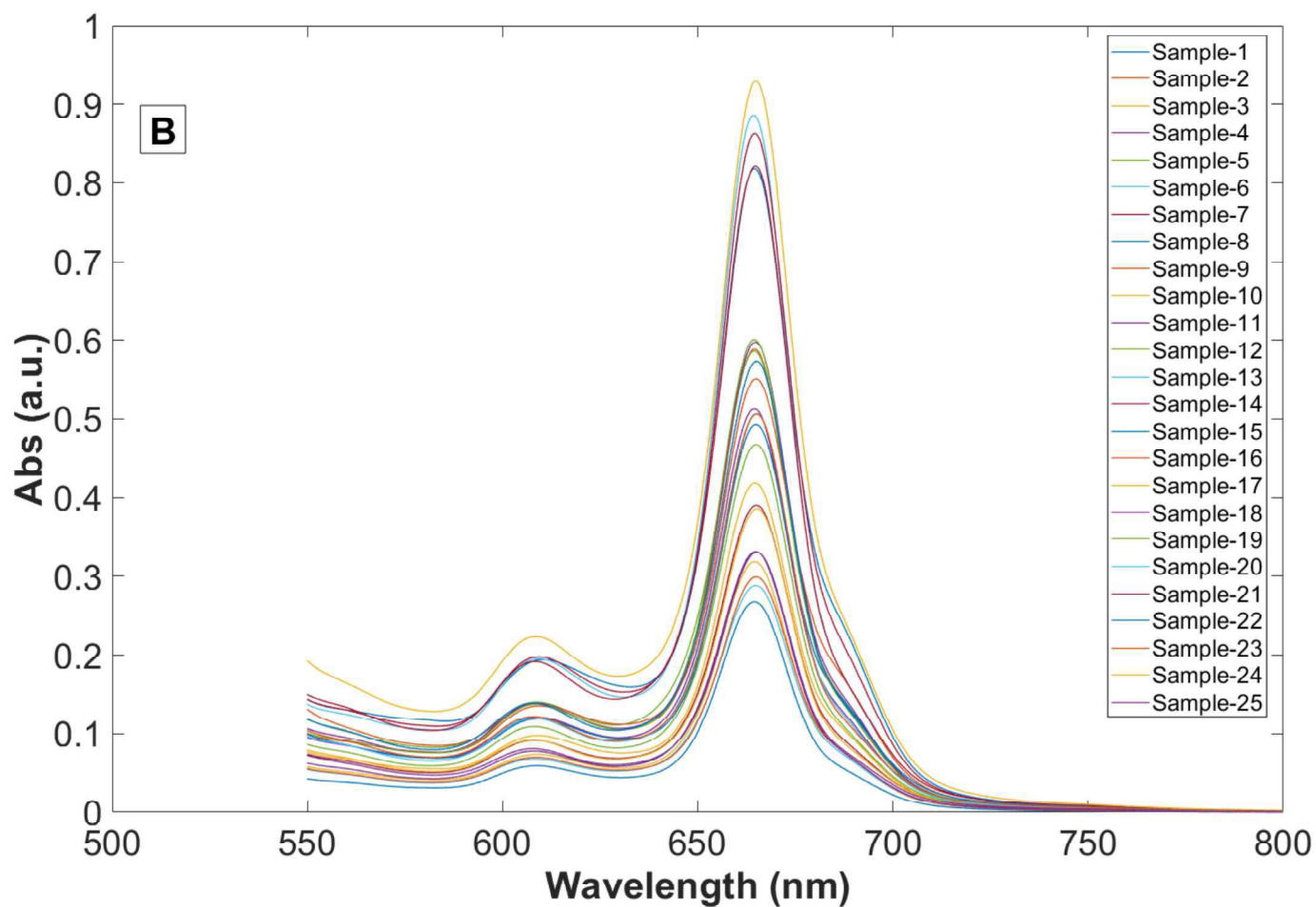
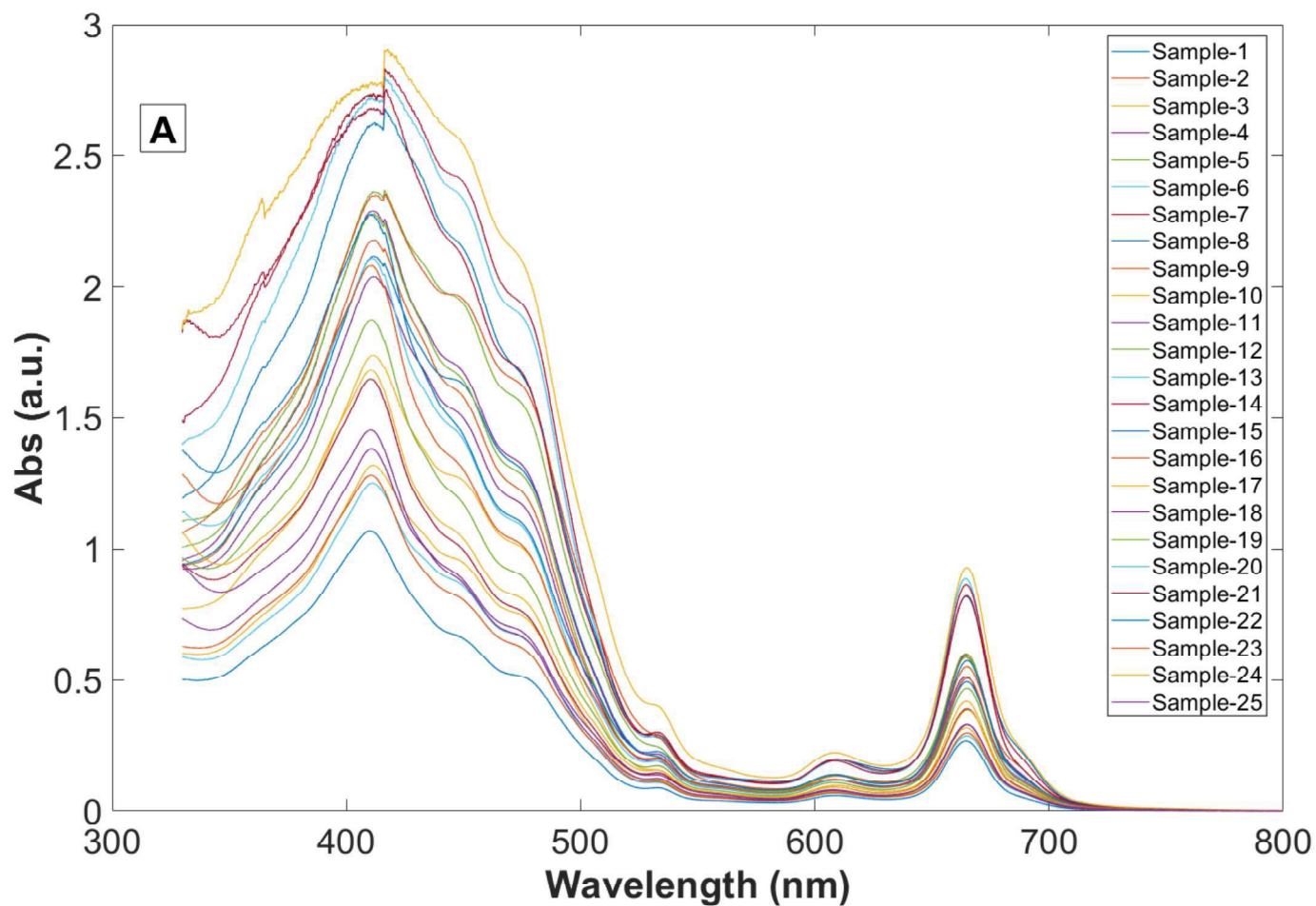
64
65

attachment to manuscript_SI_ESM7 [Click here to access/download;attachment to manuscript;ESM7.pdf](#) 

[Click here to view linked References](#)

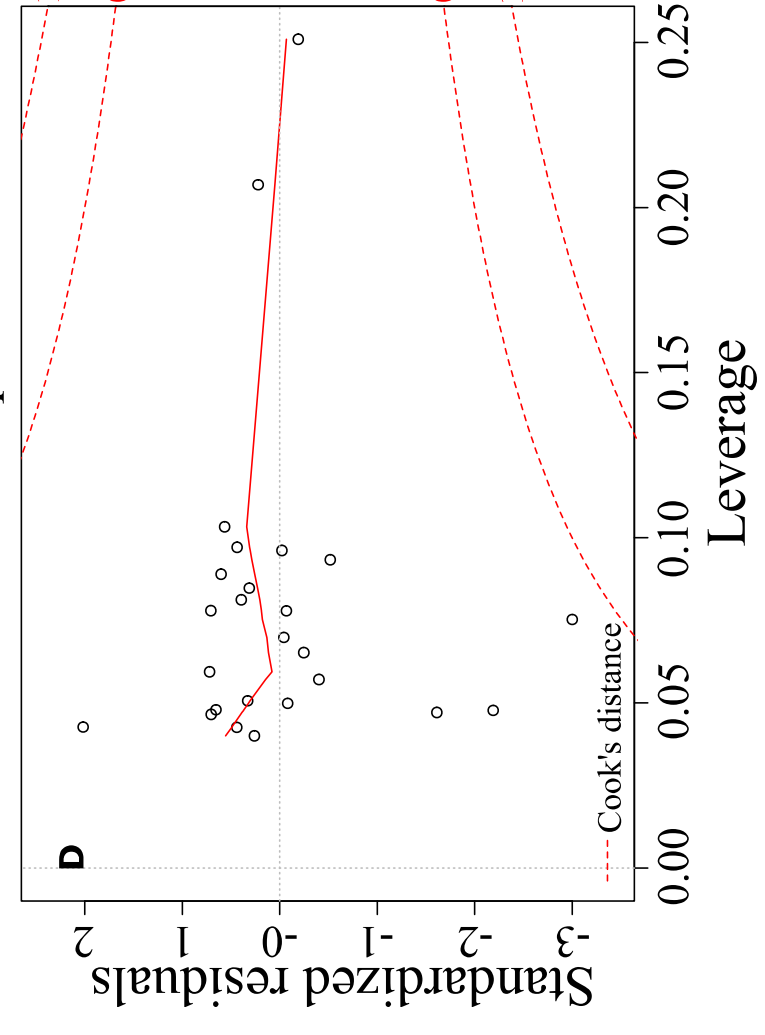
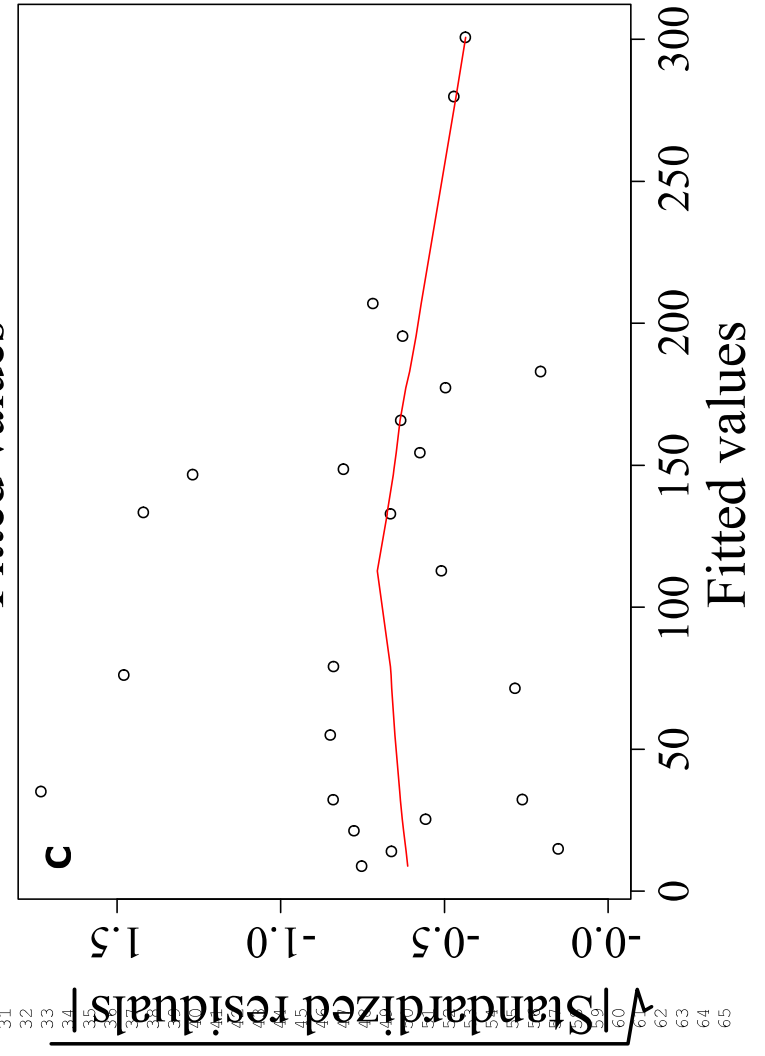
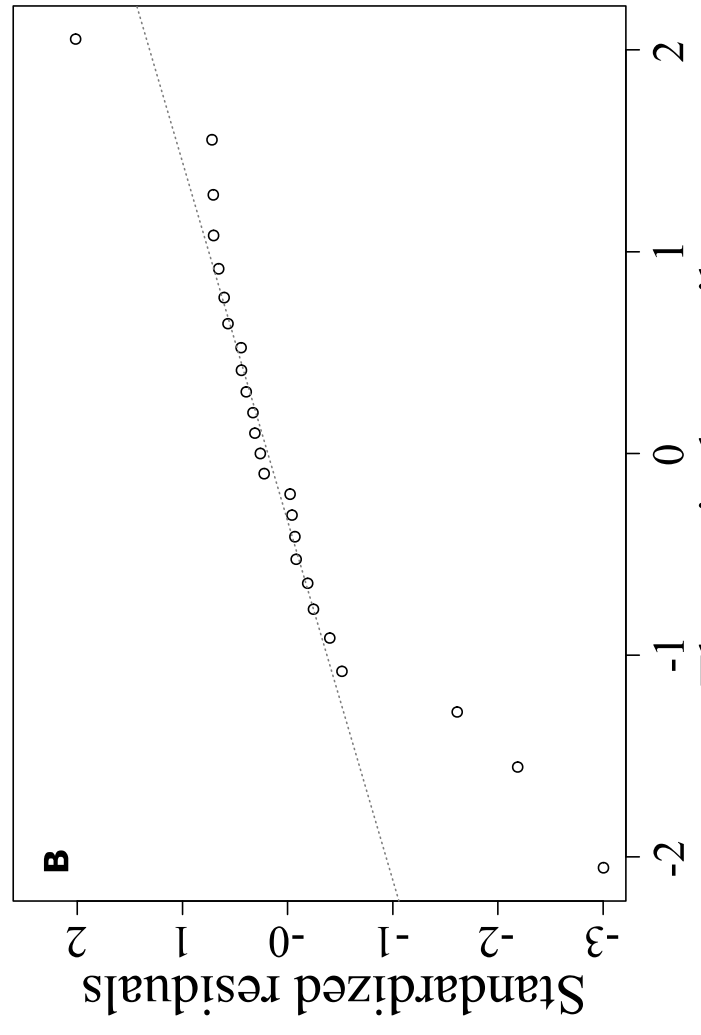
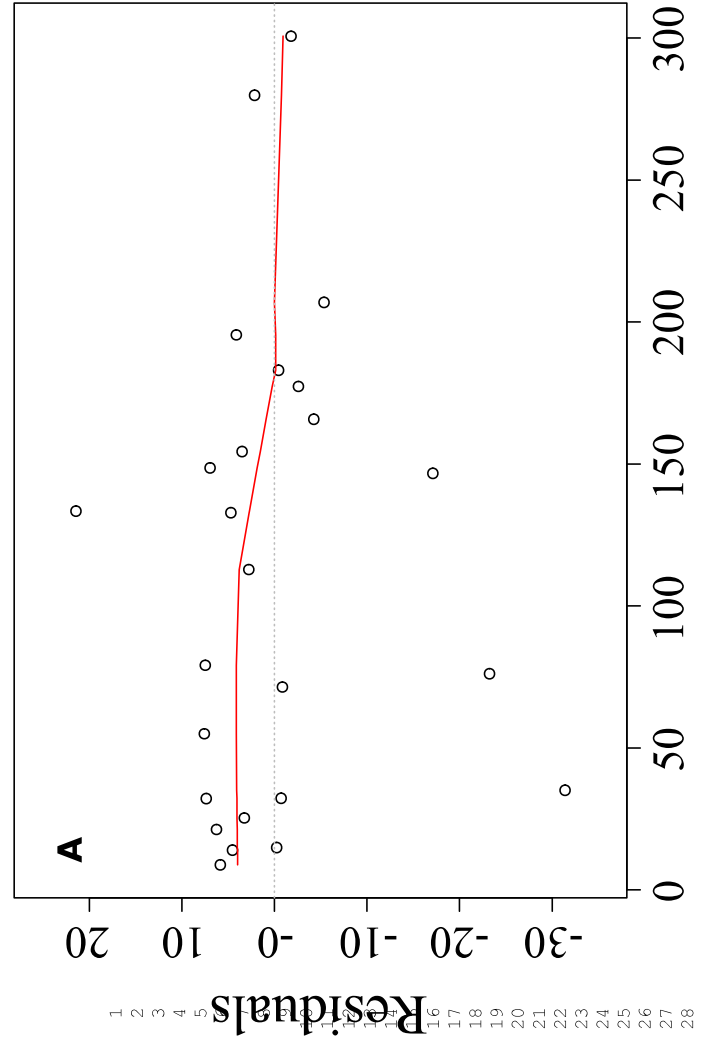
Maxima in the UV-VIS absorption spectra of target pigments					
	chl <i>a</i>	chl <i>b</i>	pyropheide <i>a</i>	phytin <i>a</i>	phide <i>a</i>
Solvent:					
Acetone					
100%					
λ_{\max} (nm)	431.1, 662.4	458.0, 645.7	410, 666.5	409.7, 665.7	410.2, 666.2
ϵ (λ_{\max})	96048, 78750	130499,	75876, 44721	100350,	97733,
(1 M ⁻¹ cm ⁻¹)		47028		44600	44251





1
2
3
4
5
6
7
8
9
10
11
12
13
14
15
16
17
18
19
20
21
22
23
24
25
26
27
28
29
30
31
32
33
34
35
36
37
38
39
40
41
42
43
44
45
46
47
48
49
50
51
52
53
54
55
56
57
58
59
60
61
62
63
64
65

[Click here to view linked References](#)



1
2
3
4
5
6
7
8
9
10
11
12
13
14
15
16
17
18
19
20
21
22
23
24
25
26
27
28
29
30
31
32
33
34
35
36
37
38
39
40
41
42
43
44
45
46
47
48
49
50
51
52
53
54
55
56
57
58
59
60
61
62
63
64
65

1

2

3

4

5

6

7

8

9

10

11

12

13

14

15

16

17

18

19

20

21

22

23

24

25

26

27

28

29

30

31

32

33

34

35

36

37

38

39

40

41

42

43

44

45

46

47

48

49

50

51

52

53

54

55

56

57

58

59

60

61

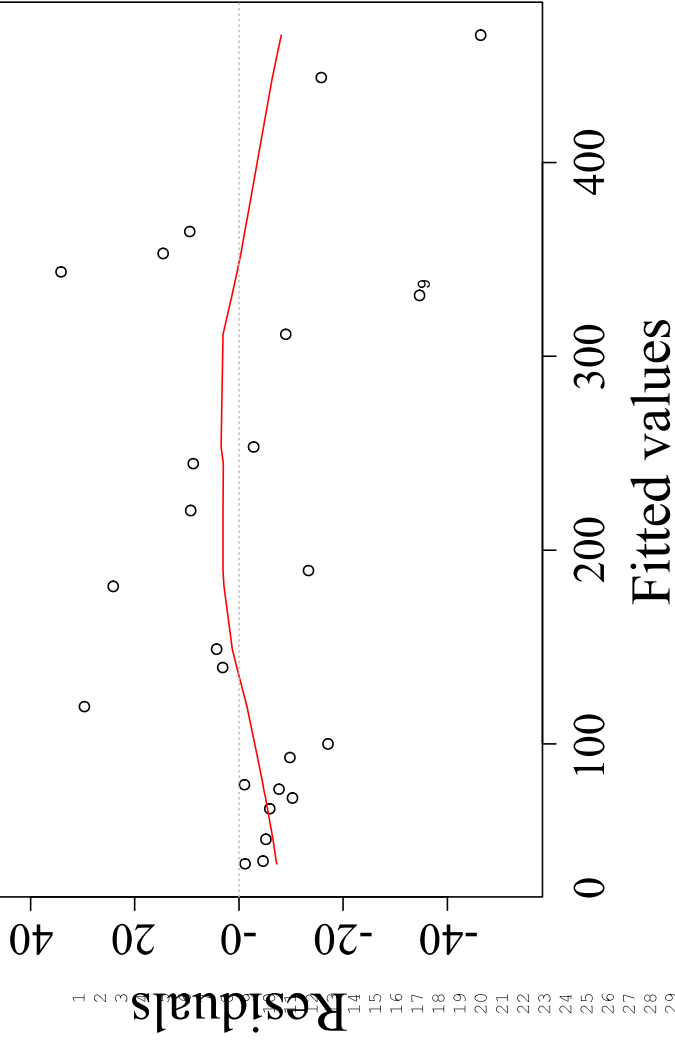
62

63

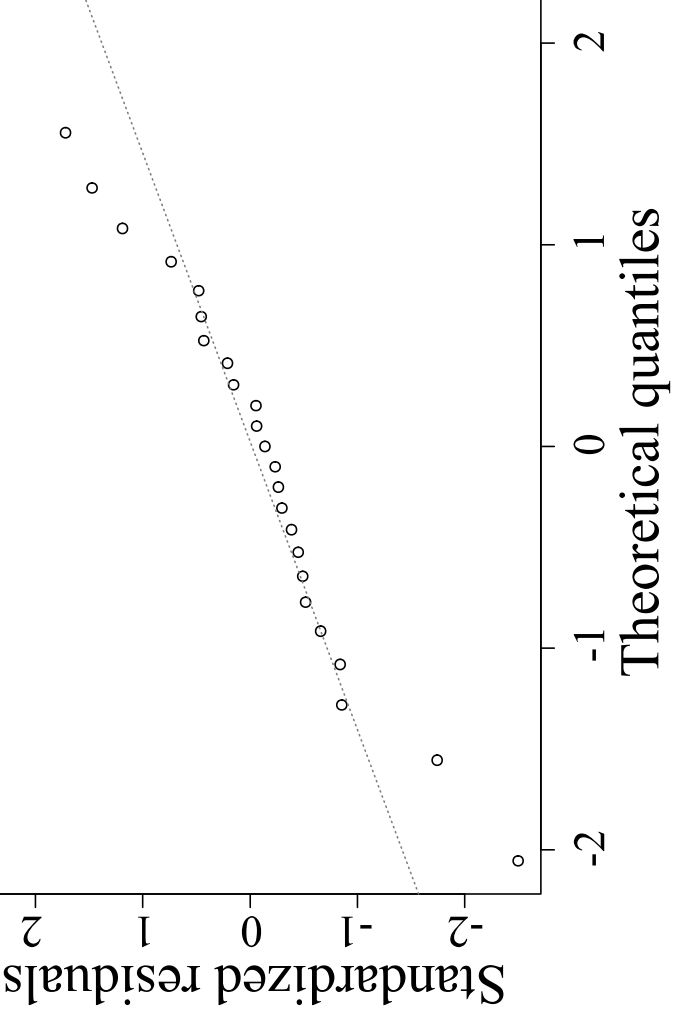
64

65

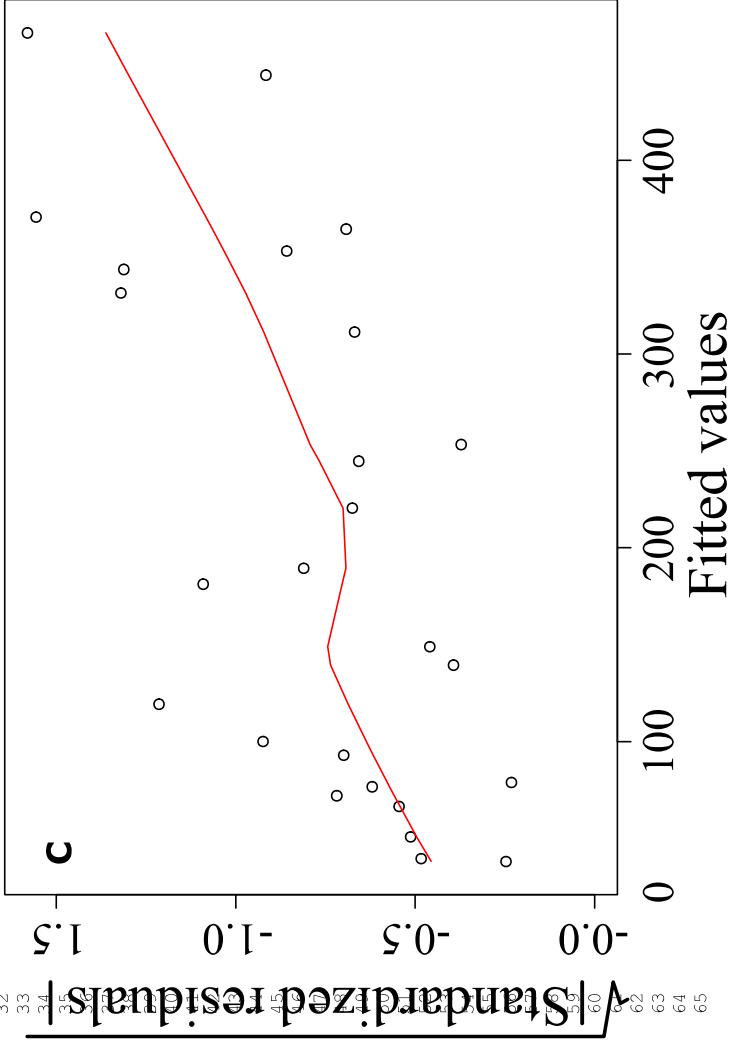
A



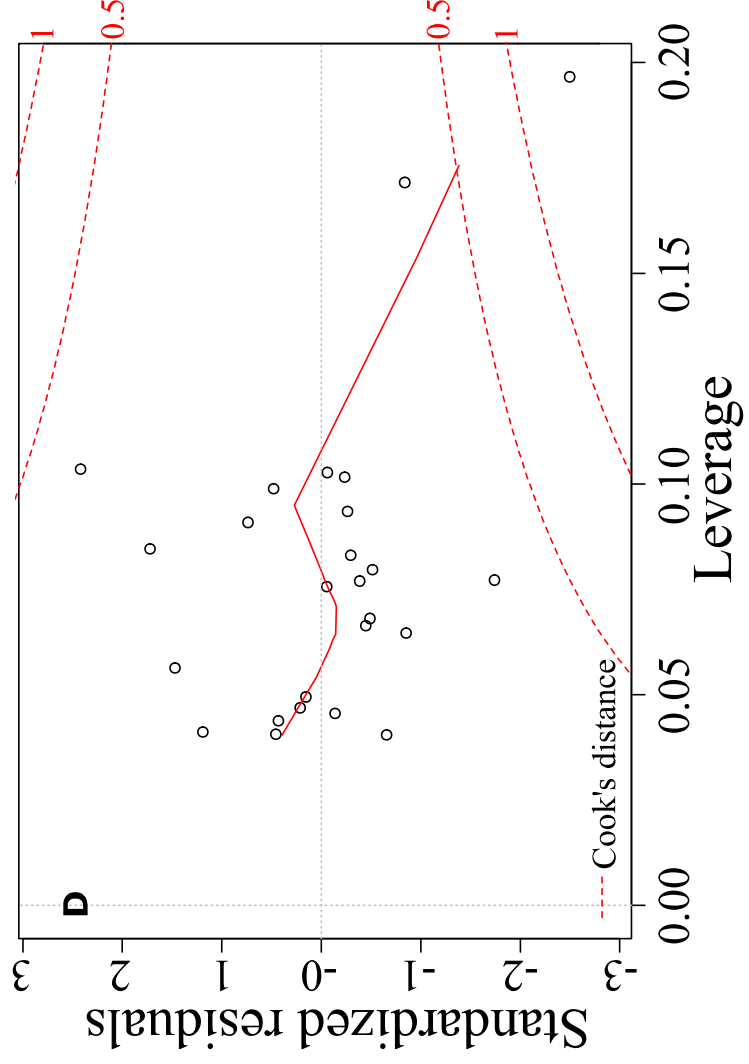
B

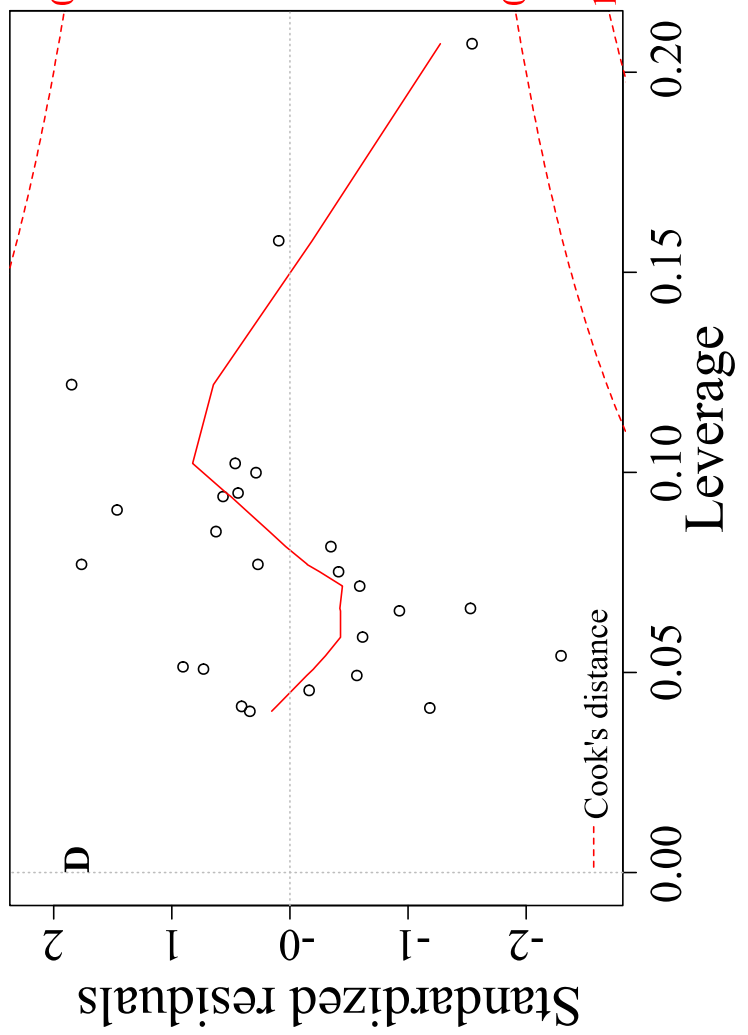
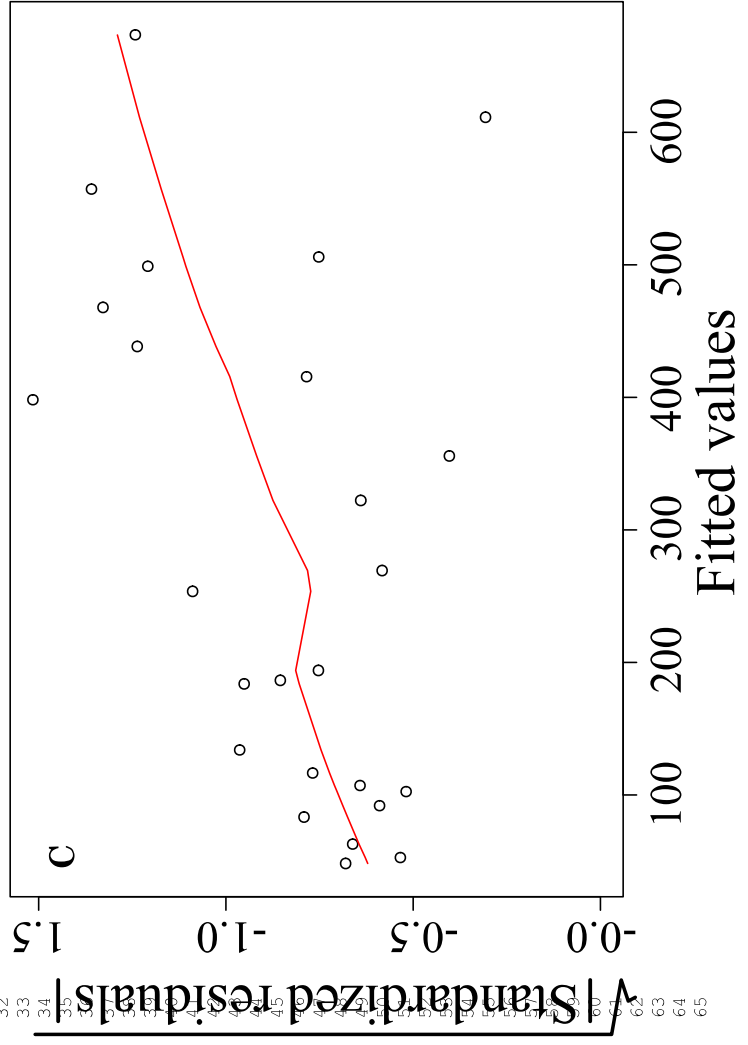
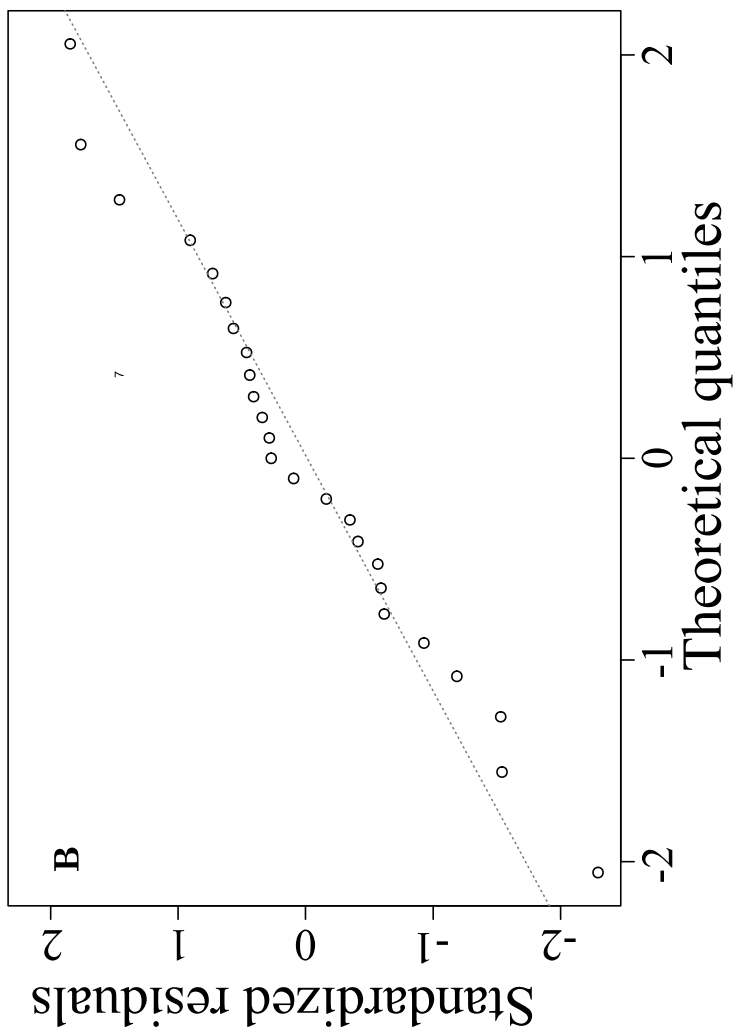
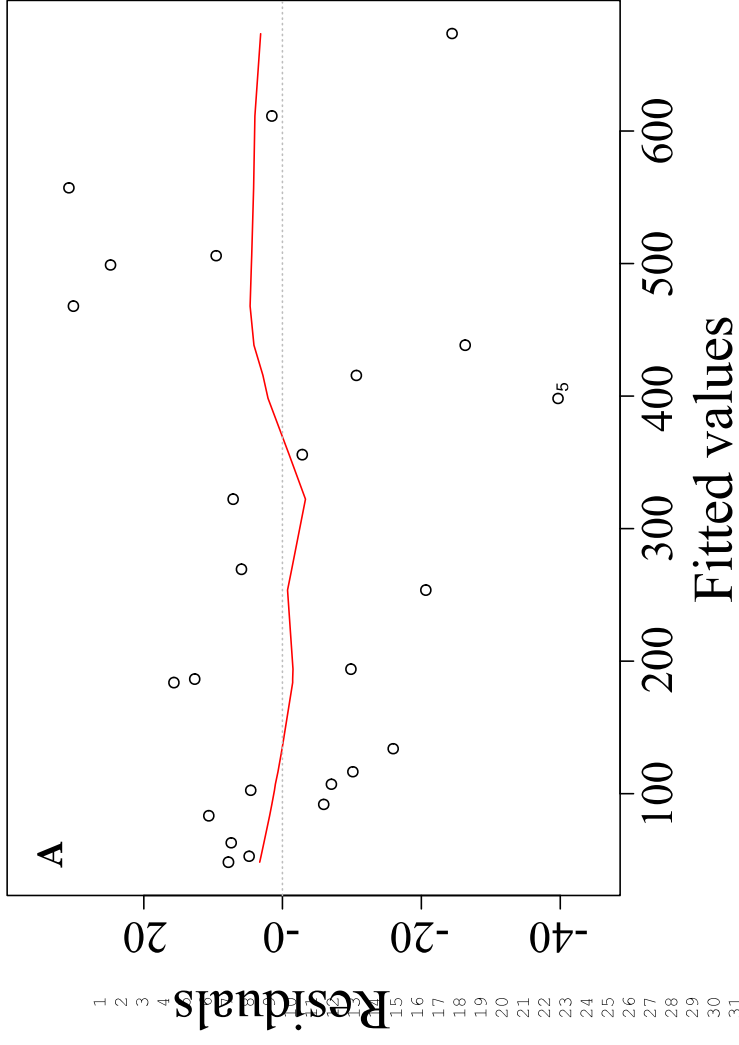


C



D





1
2
3
4
5
6
7
8
9
10
11
12
13
14
15
16
17
18
19
20
21
22
23
24
25
26
27
28
29
30
31
32
33
34
35
36
37
38
39
40
41
42
43
44
45
46
47
48
49
50
51
52
53
54
55
56
57
58
59
60
61
62
63
64
65

